AD-A250 554

# MENTATION PAGE

Form Approved
OMB No 0704-0188

is estimated to average 1 hour per response, including the time for reviewing instructions, searching existing data sources, gathering and maintaining the data needed, and completing and reviewing the collection of information. Send comments regarding this burden estimate or any other aspect of this collection of information, including suggestions for reducing this burden, to Washington Headquarters Services, Directorate for information Operations and Reports, 1215 Jefferson Davis Highway, Suite 1204, Arlington, VA 22202-4302, and to the Office of Management and Budget, Paperwork Reduction Project (0704-0188), Washington, DC 20503

| 1. AGENCY USE ONLY (Leave blank) | 2. REPORT DATE | 3. REPORT TYPE AND DATES COVERED |
|---|---|---|
| | 1991 | THESIS/DISSERTATION |

4. TITLE AND SUBTITLE
Laboratory Determination of Gas-Side Mass Transfer Coefficients Applicable to Soil Venting Systems for Removing Petroleum Hydrocarbons from Vadose Zone Soils

5. FUNDING NUMBERS

6. AUTHOR(S)
Michael E. Van Valkenburg, Captain

7. PERFORMING ORGANIZATION NAME(S) AND ADDRESS(ES)
AFIT Student Attending: South Dakota School of Mines and Technology

8. PERFORMING ORGANIZATION REPORT NUMBER
AFIT/CI/CIA- 91-137

9. SPONSORING/MONITORING AGENCY NAME(S) AND ADDRESS(ES)
AFIT/CI
Wright-Patterson AFB OH 45433-6583

10. SPONSORING/MONITORING AGENCY REPORT NUMBER

11. SUPPLEMENTARY NOTES

12a. DISTRIBUTION/AVAILABILITY STATEMENT
Approved for Public Release IAW 190-1
Distributed Unlimited
ERNEST A. HAYGOOD, Captain, USAF
Executive Officer

12b. DISTRIBUTION CODE

13. ABSTRACT (Maximum 200 words)

DISTRIBUTION STATEMENT A
Approved for public release;
Distribution Unlimited

DTIC
ELECTE
MAY 11 1992
S D

| 14. SUBJECT TERMS | 15. NUMBER OF PAGES 78 |
|---|---|
| | 16. PRICE CODE |

| 17. SECURITY CLASSIFICATION OF REPORT | 18. SECURITY CLASSIFICATION OF THIS PAGE | 19. SECURITY CLASSIFICATION OF ABSTRACT | 20. LIMITATION OF ABSTRACT |
|---|---|---|---|
| | | | |

# LABORATORY DETERMINATION OF GAS-SIDE MASS TRANSFER COEFFICIENTS APPLICABLE TO SOIL VENTING SYSTEMS FOR REMOVING PETROLEUM HYDROCARBONS FROM VADOSE ZONE SOILS

by

Michael E. Van Valkenburg

A thesis submitted to the Graduate Division

in partial fulfillment of the requirements

for the degree of

MASTER OF SCIENCE IN CIVIL ENGINEERING

SOUTH DAKOTA SCHOOL OF MINES AND TECHNOLOGY

RAPID CITY, SOUTH DAKOTA

1991

92 5 01 040

92-11972

Prepared by:

Degree Candidate

Approved by:

Major Professor

Head, Department of Civil Engineering

9/17/91

Dean, Graduate Division

## Acknowledgements

The author wishes to thank the Air Force Engineering and Services Center (AFESC), Tyndall Air Force Base, Florida, the South Dakota School of Mines and Technology, and Dr. Henry V. Mott for the opportunity to work on this project and for the financial support provided. The author would like to especially thank Dr. Mott for his hours of technical assistance and personal discussions, encouragement, and for the planning of this project.

Appreciation is also due to Dr. Thomas P. Propson, Dr. Wendell H. Hovey, and Dr. Robert W. Looyenga for serving on the graduate committee; to Bryant L. Davis for his help in characterizing the geometry of the soil particles; the staff of the Civil Engineering Department, especially Kathy Fishbach, for having helped in innumerable ways; to Doyle Heisler for his help with the data acquisition system; to Scott R. Matthew for his assistance in conducting the experiments; and last, but certainly not least, to Charles F. Schilling, Jr. His help and tactful advice, given both in the office and during our many "off-station" lunches, were always there whenever asked for.

Accession For
NTIS GRA&I ☑
DTIC TAB ☐
Unannounced ☐
Justification
By
Distribution/
Availability Codes
Dist | Avail and/or Special
A-1

QUALITY INSPECTED 4

# TABLE OF CONTENTS

# LIST OF TABLES

## LIST OF FIGURES

# CHAPTER 1

# INTRODUCTION

## 1.1 PERSPECTIVE

Contamination of the subsurface environment by organic solvents has become a national problem. The EPA's Superfund list (40 CFR Part 300, 1990) continues to grow, with continual discovery of new hazardous waste sites. Various techniques are employed to remediate these sites, including: 1) excavation and removal of the contaminated soil for proper disposal; 2) pumping and treatment of contaminated ground water and an organic phase if present; 3) containment by slurried soil-bentonite cut-off barriers; 4) *in situ* biological treatment of the organic wastes; and 5) vadose zone soil venting for gas absorption of volatiles. Each technique, or combination, may have merit at a given site. The soil venting process, an inexpensive but relatively successful technique for removal of contaminants from the vadose (unsaturated) zone, is the focus of this research.

Studies have been conducted to determine and model the actual physical processes involved in the migration of organics in the subsurface (Baehr and Corapcioglu, 1984, Sleep and Sikes, 1989, Hutzler et al. 1989a, Hunt and Sitar, 1988). Numerous scenarios of soil venting use have proved to be successful (Hutzler et al., 1989b, Downey and Elliot, 1989, Agrelot, 1985). The overall physical process of soil venting was described by Johnson et al. (1990). These authors have not considered mass transfer limitations associated with adsorption and desorption, with absorption and with the volatilization process. Most models assume that local equilibrium exists among the various phases present. Studies to determine the actual magnitudes of mass transfer

coefficients and therefore, to quantify limitations to mass transfer, are necessary either to support this assumption of local instantaneous equilibrium or to suggest an alternative.

The goals of this study are to develop a laboratory system to perform such investigations, and to provide some estimations of the magnitude of typical gas-side mass transfer coefficients applicable to soil venting systems.

## 1.2 OBJECTIVES

A prerequisite to this entire study is the successful design of a laboratory scale system to model the soil venting process. This includes the design of a soil column, incorporation of the column into a flow- through system, interfacing the experimental system with analytical measuring devices, and proving the applicability of the system. Analytical devices include pressure transducers and a gas chromatograph.

This project is designed as a fundamental analysis of mass transfer coefficients and associated interfacial surface areas applicable to systems approximating those to which soil venting is applied for the removal of petroleum hydrocarbons. Knowledge regarding these parameters will allow more accurate predictions regarding the potential for success of soil venting at a given site. Bulk contaminants are easily removed from sandy soils by soil venting procedures. Conversely, the capability of soil venting for removal of such contaminants from fine-grained soils has yet to be determined; this project focused on fine silica sands of known composition and geometry. The following specific objectives were addressed:

1. Development of a system to adequately study the removal of hydrocarbons for laboratory soil beds;

2. Determination of the suitability of the laboratory design to current and future work involving similar study areas;

3. Evaluation of overall mass transfer coefficients for a single component systems as a function of the mass of the solute remaining in the soil column and the interstitial velocity of the transporting vapor phase.

4. Estimation of mass transfer correlation parameters.

## 1.3 APPROACH

The approach applied to meet objective 1 consisted of the design and fabrication of a soil column capable of approximating actual soil systems, through which a convective air phase could be passed to volatilize an organic solute. The resulting off-gas was routed to a gas chromatograph for off-gas characterization. It was necessary that this soil column and the flow paths before and after it be part of a closed system in order that a mass balance could be closed upon the system. This data acquisition system included the measurement of the flow rate of air with a calibrated rotameter and the measurement of system pressures at various locations. Repeated measurement of pressure required the use of electrical pressure transducers. Transducer output was sent through a data acquisition system to a computer file for use in data analysis.

Objective 2 was addressed on the basis of the results of this study. Success of the data collection, closure of the mass balance and other experimental results were the determining factors in assessing whether or not this objective was met.

The approach applied to meet objective 3 consisted of a series of experiments using three soils of different grain size through which air

was forced at various flow rates to remove liquid heptane by volatilization. Off-gas concentration profiles versus time were obtained for each run. These clearly suggested the occurrence of various behavioral regions. These profiles of off-gas concentration versus time led to statistically derived relationships between the apparent overall mass transfer coefficient ($k_v a$) and a modified Reynolds number (Re').

# CHAPTER 2

# THEORY AND BACKGROUND

## 2.1 SUCCESS OF THE SOIL VENTING PROCESS

Numerous full and pilot-scale studies have shown soil venting to be effective for the removal of volatile organic contaminants (VOCs) from vadose zone soils. For the most part these soils have been comprised mostly of sands and gravels and the contaminants removed range from n-hexane to the relatively non-volatile, heavier components of JP-4 jet fuel (Agrelot, et al., 1985; Bennedson, et al., 1985; Brown, et al., 1988; EPA, 1989a; EPA, 1989b; Mutch, et al., 1989; DePaoli, et al., 1989; Hutzler, et al., 1989b). In one particular case (EPA 1989a) it was shown that VOCs can apparently be removed from stiff clay soils by soil venting. It was suggested that soils of low permeability to water transport may be effectively remediated by soil venting given that sufficient vapor phase void volume exists within the pore structure of the medium. Additional study was suggested. Two most important parameters contributing to the success of soil venting, then, are the volatility of the contaminants in question and the ease of vapor phase transport within the soil.

## 2.2. PHENOMENA INVOLVED IN THE SOIL VENTING PROCESS

Overall transport of VOCs in the vadose zone may be due to or influenced by any one or combination of numerous processes including: 1) convection (advection) within the vapor phase; 2) dispersion or mechanical mixing associated with vapor phase convection; 3) molecular diffusion within the vapor phase; 4) convection with a mobile liquid phase; 5) adsorption from the vapor phase; 6) adsorption from the liquid phase; 7) volatilization from aqueous phase liquid, non-aqueous

phase liquid (NAPL) or dense, non-aqueous phase liquid (DNAPL); and, 8) transformations by biological or chemical processes. Of these processes, volatilization and vapor phase convection are exploited in soil venting applications to provide for the removal of VOCs from vadose zone soils. Soil venting, or vapor extraction, is an *in situ* gas absorption process which exploits the volatility of target compounds. Chemical components having large vapor pressures will tend to volatilize from a NAPL or DNAPL into a continually replenished vapor phase more rapidly than those having lower vapor pressure. Similarly, those components with high Henry's Law constants will tend to volatilize from aqueous solution into a continually replenished vapor phase more rapidly than those having lower Henry's Law constants.

Volatilization must occur across the vapor/liquid interface. It is known that an equilibrium condition occurs between the liquid and vapor phase monolayers situated on either side of this interface (Treybal, 1980; Henley and Seader, 1981). This equilibrium condition may be used to describe mass transfer, believed to occur due to molecular diffusion across the interface, in terms of boundary layer (or film) theory. The interface may be represented by two stagnant boundary layers situated on either side of the interface. Mass transfer across the interface occurs by molecular diffusion through these respective layers. These boundary layers constitute resistances in series, each contributing to the overall mass transfer resistance of the interface. The direction of transport in soil venting processes is from the liquid, across the liquid and vapor boundary layers, and then into the bulk vapor phase. Hence, the "two film" theory is often necessary to describe mass transfer across such interfaces in terms of

both local and overall mass transfer coefficients and both local and overall driving potentials.

Convection within the vapor phase basically acts to carry away the constituents that have been transported through the series resistances and to maintain a departure from equilibrium between the bulk liquid and bulk vapor phases. If these two phases fully equilibrate, net transfer ceases. Additionally, the rate of convection determines the velocity of the vapor relative to the interface and can affect the thickness of and, thus, the magnitude of the mass transfer resistance offered by the vapor side boundary layer.

The total surface area across which the mass transport occurs is important with respect to the overall rate of contaminant removal. Ideally, the total rate of removal will be directly dependent upon the vapor/liquid interfacial area. Interaction at the molecular level of NAPL and DNAPL with the solid phase surface can be important in determining both the geometry and specific surface area of the interface. Specific interfacial surface area is usually expressed as area per bulk unit volume of the porous medium.

A NAPL or DNAPL that has contaminated a site will typically be comprised of several components, most commonly gasoline, JP-4, or mixtures of solvents. When soil venting is initiated, components comprising these mixtures are volatilized at rates dependent upon the relative volatility, liquid and vapor phase diffusivities, and liquid phase fugacity of each component. The vapor phase is generally considered to be an ideal solution. Conversely, in liquid mixtures of components that interact with each other or are chemically dissimilar, the activity of each component will either be greater than or less than

the corresponding concentration. The liquid phase activity coefficient then becomes important in describing the condition at the vapor/liquid interface. Generally, in a multi-component system, components will be removed in the order of volatility. Highly volatile components are removed first, followed by those that are less volatile as found by Marley and Hoag (1984). Certain of the heavy components of JP-4 or diesel fuel can be quite resistant to removal by soil venting.

In order to fundamentally describe the soil venting process in soils of low permeability (or in any soil), the three major phenomena discussed above--vapor phase convection, interfacial mass transfer, and vapor/liquid equilibrium--deserve the major emphasis. These three phenomena are discussed further in ensuing paragraphs.

2.2.1 Vapor Liquid Equilibria (VLE)

As previously mentioned, an equilibrium condition is established between the liquid and vapor phases at the vapor/liquid interface during a mass transfer process. This condition within these respective monolayers discussed above may be described thermodynamically as:

$$f_{i,l} = f_{i,v} \text{ ;or } [f^{\circ}_i \gamma_i X_i]_l = [f^{\circ}_i \gamma_i Y_i]_v \qquad (2.1)$$

where: $f_i$ = the partial fugacity of component i;
$f^{\circ}_i$ = the reference state fugacity (pure component at temperature and pressure of system) of component i;
$\gamma_i$ = the activity coefficient of component i;
$X_i$ = the liquid phase mole fraction concentration of component i;
$Y_i$ = the vapor phase mole fraction concentration of component i;
l = denotes the liquid phase; and,
v = denotes the vapor phase.

At the environmental temperatures and pressures encountered in systems to which soil venting would be applied, fugacity coefficients (fugacity divided by the pressure) approach unity; thus, the reference state

fugacity of a component of the NAPL approaches the vapor pressure of the pure component. Correspondingly, the reference state fugacity of a component of the vapor approaches the system pressure. The vapor phase is generally considered to be an ideal solution ($\gamma_{iv}$ = unity), and upon inclusion of these modifications and application of Dalton's Law, Equation 2.1 becomes:

$$[P^{\circ}_i \gamma_i X_i]_l = P_T Y_i \qquad (2.2)$$

where: $P^{\circ}_i$ = the liquid vapor pressure of component i; and,
$P_T$ = the total system pressure.

Vapor pressure data for individual components is readily available in handbooks (CRC, 1989; Perry et al., 1984) or may be estimated from various empirically calibrated relationships (Grain, 1990). Activity coefficients for components in non-ideal mixtures can be estimated from solution theory; however, such estimates may be greatly in error. Consequently, empirical measurement is generally necessary to obtain accurate values of $\gamma_{il}$ over the potential range of applicability. For ideal (or nearly ideal) solutions, Raoult's Law and Henry's Law may be used to describe the solvent and solute VLE, respectively. Raoult's Law may be stated as:

$$P^{\circ}_{il} X_i = P_T Y_i \qquad (2.3)$$

where $\gamma_{il}$ is taken as unity. Henry's Law may be stated as:

$$H_i X_i = P_T Y_i \qquad (2.4)$$

where the Henry's constant, $H_i$, is the product of $\gamma_{il}$ and $P^{\circ}_{il}$. The liquid phase activity coefficient may be estimated from UNIFAC (Arbuckle, 1983). For dilute solutions, activity coefficients can be estimated by equating the partial fugacities for two non-miscible liquid phases (Lyman, 1990):

$$\gamma_i = 1/S_i \qquad (2.5)$$

where $S_i$ represents the solubility of component i in the solvent.

The assumption of a constant activity coefficient is necessary to applications of Henry's Law; thus, it is applicable only to situations that closely approximate the infinitely dilute case. For most mixtures of petroleum hydrocarbons in water, Henry's Law is applicable due to the low solubilities of these compounds in water.

Certain of the components comprising complex mixtures such as gasoline, diesel fuel and JP-4 are dissimilar in chemical properties, and these mixtures would be expected to behave as non-ideal mixtures. Marley and Hoag (1984) successfully described the removal of gasoline from a laboratory column by soil venting using the ideal solution assumption. In addition, effluent profiles of single solute experiments using benzene agreed well with calculated profiles assuming that local equilibrium conditions exist. However, their study involved the measurement of solute vapor concentrations at the end of a long (65 cm) experimental soil column. Additional study at the laboratory scale is warranted using single component and binary mixtures in thin soil columns to either further reinforce this finding or suggest the alternative.

Johnson et al. (1989) assumed that local equilibrium exists between the vapor, free-liquid, sorbed, and dissolved phases during soil venting operations. This assumption was based on a calculation of the distance required for air to become saturated with contaminant vapors after entering a contaminated region. Their calculation was based on the mass transfer model between two infinite flat plates. Assuming negligible dispersion in the direction of flow (the z

direction) the governing equation for the vapor phase concentration, C, is:

$$u_v \left[\frac{\partial C}{\partial z}\right] = D_x \left[\frac{\partial^2 C}{\partial x^2}\right] \qquad (2.6)$$

where: $u_v$ = the vapor velocity in the z direction ($Lt^{-1}$);
$D_v$ = the vapor phase molecular diffusivity ($L^2t^{-1}$);
x = the coordinate perpendicular to the plates; and,
z = the coordinate in the direction of flow.

The solution by Johnson et al. (1989) predicts that the vapor phase concentration reaches 99% of its equilibrium value at the centerline between the two plates after the vapor has traveled a distance:

$$z = 2u_v L^2/D \qquad (2.7)$$

where L is half the plate separation distance (analogous to the pore radius). Typical values of these parameters in soil venting operations are $u_v$ = 1 cm/sec, L = 0.10 cm, and D = 0.10 $cm^2$/sec. The typical distance to reach equilibrium as calculated by Equation 2.7 is then 0.05 cm, suggesting that the local equilibrium assumption is appropriate. The channels in porous media are not flat plates and the organic phase is not necessarily continuous; therefore, actual soil systems could behave differently than this model predicts.

### 2.2.2 Mass Transfer Across the Interfacial Surface Area

Marley and Hoag (1984) suggested that the vapor/liquid system within a soil column being vented with air can accurately be described by assuming that a local equilibrium exists between the respective phases. Given a sufficiently long column, the off-gas can approach equilibrium with the liquid near the outlet of the column. Assumption of an equilibrium condition throughout the porous medium implies that the net rate of transport across the interface is zero. A fundamental

study to determine the magnitude of mass transfer coefficients is warranted.

Concentration profiles in the vicinity of the interface between an organic liquid and an associated vapor phase within a system approximating a gas absorption column being operated under stationary conditions is represented schematically in Figure 2.1. Diffusive flux of component i across the interface, $F_i$, is described by Fick's first law:

$$F_{iv} = -D_{iv}\rho_v \partial Y/\partial z \quad ; \quad F_{il} = -D_{il}\rho_l \partial X/\partial z \tag{2.8}$$

where: $F_i$ - the molar flux of component i ($ML^{-2}t^{-1}$);
$D_i$ - the diffusivity of component i in the phase in question;
$\rho$ - molar density of the respective phase; and,
X,Y - liquid, vapor mole fraction concentrations.
z - coordinate in the direction of mass transfer.

Under stationary conditions the magnitude of the flux of component i must be identical across each of the resistances, such that $F_{iv}$=-$F_{il}$=$F_i$. If the thickness of the liquid and vapor boundary layers are taken to be $\delta_l$ and $\delta_v$, respectively, and each gradient is approximated to be linear as a consequence of attaining a "quasi" steady state, a mass transfer coefficient, $k$, may be defined as $D_i/\delta$, and Equation 2.8 may be restated as:

$$F_i = \rho_v k_v (Y^*_i - Y_i) = \rho_l k_l (X_i - X^*_i) \tag{2.9}$$

where $X^*_i$ and $Y^*_i$ are the liquid and gas phase concentrations in the respective monolayers adjacent to the interface, considered to be related through equilibrium.

Consideration of the relationship between $X^*_i$ and $Y^*_i$, relative to an arbitrary condition $[X_i, Y_i]$ (see Figure 2.2) allows $F_i$ to be stated in terms of an overall mass transfer coefficient, **K**, and overall driving force (Treybal, 1980):

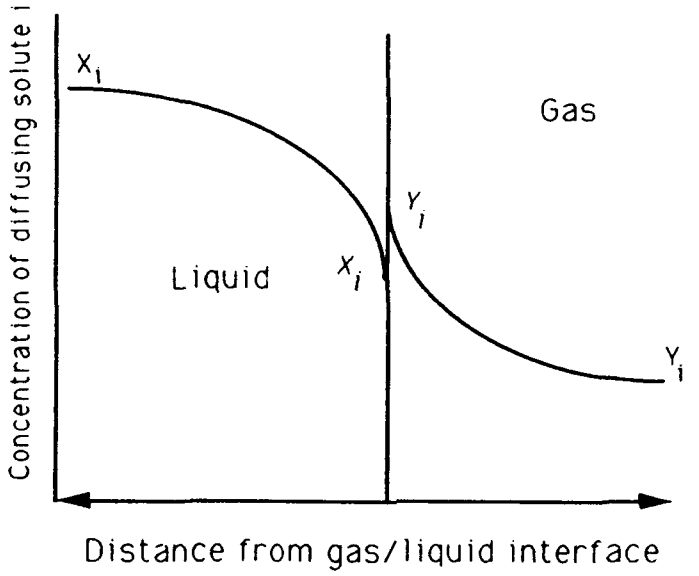


Figure 2.1: Schematic representation of the two-resistance concept: concentration profiles in the gas and liquid phases near the gas/liquid interface.

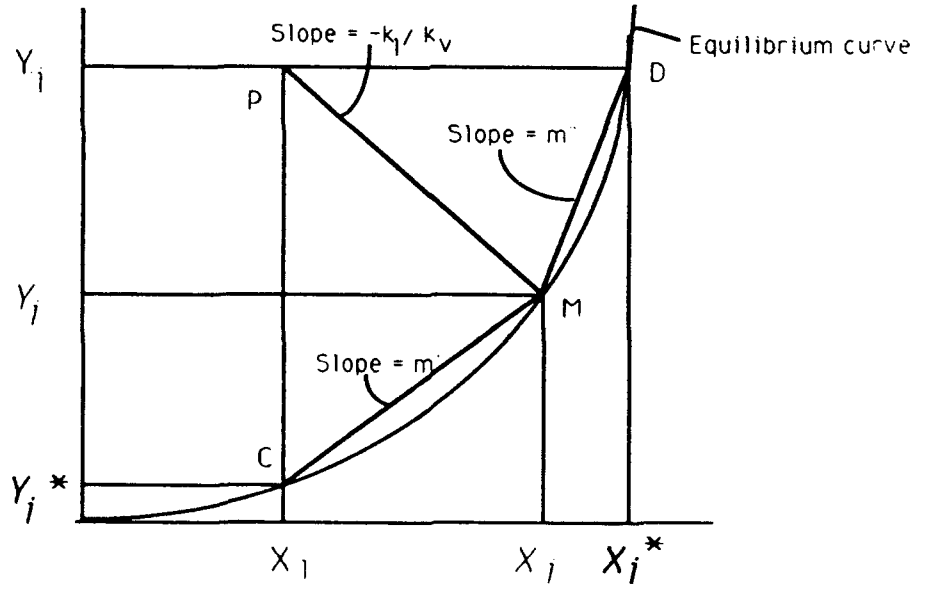


Figure 2.2: Schematic representation of the relationship between an arbitrary point with gas and liquid concentrations (Xi,Yi) and the vapor/liquid equilibrium curve for the description of overall mass transfer coefficients.

$$F_i = \mathbf{K}_v(Y^*_i - Y_i) = K_l(X_i - X^*_i) \qquad (2.10)$$

where: $1/\mathbf{K}_v = 1/k_v\rho_v + m'/k_l\rho_l$;
$1/\mathbf{K}_l = 1/m''k_v\rho_v + 1/k_l\rho_l$;
$Y^*_i$ is the $Y_i$ corresponding to $X_i$;
$X^*_i$ is the $X_i$ corresponding to $Y_i$;
$m'$ is the chord connecting the point $[X^*_i, Y_i]$ with the intersection of the equilibrium curve and the line of slope $-k_l/k_v$ originating at $[X_i, Y_i]$; and,
$m''$ is the chord connecting the point $[X_i, Y^*_i]$ with the intersection of the equilibrium curve and the line of slope $-k_l/k_v$ originating at $[X_i, Y_i]$.

Equation 2.10 describes the case for a non-linear equilibrium relationship, where the activity coefficient, $\gamma_i$, is neither unity nor constant. For cases in which Raoult's law or Henry's Law is applicable, $m'=m''=m$. For Raoult's Law, $m = P_v/P_T$ and for Henry's Law, $m = P_v\gamma_i/P_T$.

Numerous empirical correlations for specific geometries and conditions describing $k_v$ and $k_l$ may be found in the literature and are generally of the form:

$$Sh = aRe^bSc^c \qquad (2.11)$$

where: $Sh = kd/D$; $Re = u_v d/\eta$; $Sc = \eta/D$;
$d$ = a characteristic system length;
$u_v$ = the vapor velocity;
$\eta$ = the kinematic viscosity of the fluid ($L^2t^{-1}$); and,
a, b, and c are empirically determined coefficients.

In packed bed systems, the Reynolds number (Re) is often expressed as a modified Reynolds number (Re') where the average interstitial pore vapor velocity is $u_v$ and the effective pore diameter ($d_e$) is the characteristic length. The effective pore diameter in randomly packed soil systems is given by Dullien (1979) as an equivalent spherical void diameter:

$$d_e = [(\epsilon/(1 - \epsilon))d_p^3]^{1/3} \qquad (2.12)$$

where: $d_e$ = the size of a spherical void of volume equal to the local mean pore volume associated with a sphere in

the bed;
$\epsilon$ = the vapor void fraction; and,
$d_p$ = the diameter of the particles.

Variations in the vapor phase convective velocity, $u_v$, in theory should then result in corresponding variations in the magnitude of $k_v$. If the rate of mass transfer is sensitive to the convective velocity, then, it may be asserted that the vapor side resistance is, indeed, significant. Should one of the resistances be sufficiently small such that it may be neglected, the mathematical formulation is greatly simplified. Studies of only the gas side mass transfer coefficients can be accomplished by totally eliminating the liquid side resistance. This can be done by the study of the removal of only single solute compounds from an interface. Gamson et al. (1943) conducted experiments involving the evaporation of water from soaked spheres ranging in size from 0.09 to 0.456 inch in diameter. Evaporation rates, and hence mass transfer rates were measured. J-factors (a dimensionless mass transfer factor) were calculated and plotted against the Reynolds number. The results showed that the laminar flow region occurred when the Reynolds number (Re) was less than 40, the turbulent regime occurred at Re > 350, and a transition region existed in between. Gamson et al. (1943) found that the j-factor defined as:

$$j_d = \frac{k_v p_{gf} M_m}{G}\left[\frac{\eta}{D}\right]^{2/3} \qquad (2.13)$$

for mass transfer at Re < 40 could be expressed as:

$$j_d = 16.8\left(\frac{d_p u_v}{\eta}\right)^{-1} \qquad (2.14)$$

where: G = the superficial mass vapor velocity ($ML^{-2}t^{-1}$);
$M_m$ = mean molecular weight of vapor stream; and,
$p_{gf}$ = the log mean partial pressure of the non-

transferred gases in the gas film.

Equations 2.13 and 2.14 maybe combined to provide an expression for the mass transfer coefficient:

$$k_v = \frac{16.8}{P_{gf} M_m d_p} \left[ \mu \rho^2 D^2 \right]^{1/3} \qquad (2.15)$$

where $\mu$ is the absolute viscosity ($ML^{-1}t^{-1}$)

This equation supports the theory that the mass transfer coefficient is independent of the vapor velocity in the laminar flow region, but experimental data were too sparse to firmly support this theory.

Subsequent research by Wilke and Hougen (1945) improved the correlations for Reynolds numbers below 350. Experiments were similar to those of Gamson et al. (1943), but more data points were taken in the region where Re < 350. The resulting correlation smoothed out the transition between laminar and turbulent flow. Their correlation was similar to Equation 2.15:

$$k_v = \frac{1.82G}{P_{gf} M_m} \left( \frac{d_p G}{\mu} \right)^{-0.51} \left( \frac{\mu}{\rho D} \right)^{-2/3} \qquad (2.16)$$

This later correlation does show a dependance of the vapor side mass transfer coefficient on the vapor velocity.

Transport of a given contaminant from the liquid to the vapor phase must occur across the vapor/liquid interface, which is most commonly defined as interfacial area per bulk volume of porous medium, $\alpha$. A variation in the magnitude of $\alpha$ would then be expected during the process of removing a NAPL or DNAPL from vadose zone soils. An increase or decrease in the rate that a single component is removed from a given porous medium contained in a laboratory column by venting with air at constant temperature and constant air flow could be

indicative of an increase or decrease, respectively, in the magnitude of $\alpha$. Water is, in general, the original liquid in vadose zone soils contaminated with hydrocarbons. Water associates with layered silicates and with the organic matter in soils. If a hydrocarbon NAPL or DNAPL is present, it will exist as a separate phase associated with the mineral surfaces of the soil. This separate phase is most likely removed first by a convective air phase. During these initial stages the surface area for mass transfer is the $\alpha$ associated with the organic liquid phase. This area will decrease with time until all of the NAPL is removed. At this point, the hydrocarbon remaining in the vadose zone is that portion soluble in the water phase. Hydrocarbons will continue to be removed, but the interfacial surface area for mass transfer will now be dependent upon the moisture content of the soil.

If it is assumed in the absence of water that $\alpha$ is constant for a given quantity of pure-component NAPL in a given soil media, changes in the mass transfer rate should be observed corresponding with changes in the interstitial vapor velocity. Changes in the magnitude of $\alpha$ will correlate with changes in the vapor phase porosity, $\epsilon_v$; which lead to changes in the vapor phase interstitial velocity, $u_v$, and in the characteristic length, $d_e$. These parameters are associated with many correlations used to determine local and overall mass transfer coefficients. The specific interfacial surface area, $\alpha$, is perhaps the least quantitatively understood and most difficult parameter to evaluate in mass transfer systems. A fundamental study directed toward evaluating this parameter with regard to soil venting systems is highly warranted.

## 2.3 THE DIFFERENTIAL SOIL COLUMN

True soil venting systems are three-dimensional; however, given the nearly horizontal flow of air induced by capping a site and the tendency of soil systems to be stratified, systems can often be closely approximated by the assumption of horizontal vapor movement. The mathematics of these systems then becomes greatly simplified. Such models and the associated approximations must have accurate parameters to effectively simulate or predict the performance of soil venting systems. Laboratory studies directed toward fundamental research and evaluation of transport parameters must take advantage of every simplification possible to rigidly control the environment while maintaining a system representative in every way possible of the "real world" conditions. Hence, the physical system considered herein, shown schematically in Figure 2.3, is one-dimensional and comprises the soil, the liquid phase, and the vapor phase contained within a thin, small diameter laboratory column. A schematic representation of the orientation of a NAPL and the solid phase within this physical system is shown in Figure 2.4.

Application of the mass conservation law to component i in the vapor residing within the control volume bounded by the cross-sectional area of the column and the coordinates z and z+$\Delta$z, and considering that the system is under quasi-stationary conditions, such that the accumulation term may be neglected, yields:

$$-\frac{d(\epsilon_v Y_i u_v \rho_v)}{dz} + \alpha F_i \simeq 0 \qquad (2.17)$$

Application of the mass conservation law to component i and considering the liquid within the control volume defined above yields:

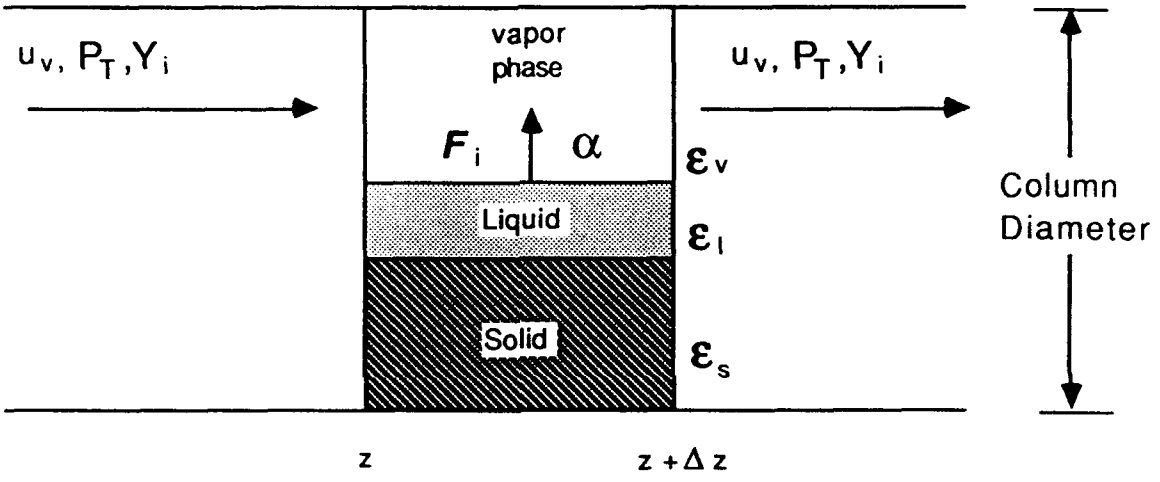


Figure 2.3: Schematic representation of mobile and stationary phases within a differential element in a one dimensional soil column.

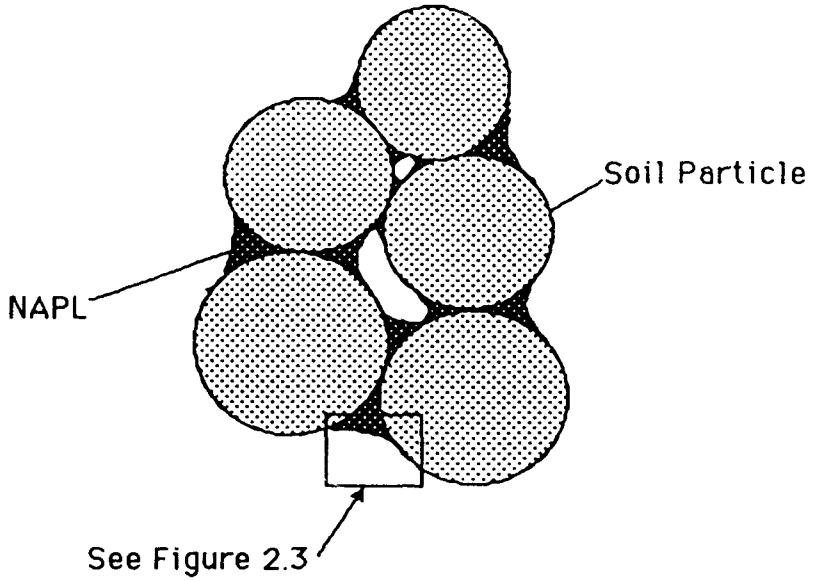


Figure 2.4: Micro-scale schematic of an actual solid/liquid/vapor interface at the soil particle level.

$$\frac{d(\epsilon_l X_i \rho_l)}{dt} + \alpha F_i \simeq 0 \qquad (2.18)$$

Application of the mass conservation law to the total quantity of vapor within the control volume and assuming quasi-stationary conditions yields:

$$-\frac{d(\epsilon_v u_v \rho_v)}{dz} + \alpha \Sigma F_i \simeq 0 \qquad (2.19)$$

The vapor density and system pressure at ambient temperature may be related at environmental temperatures and pressures through the ideal gas law, and the vapor and liquid porosities are related by summing the contributions of the three distinct phases, such that $\epsilon_v+\epsilon_l+\epsilon_s=1.0$. The remaining equation, given in integral form describes the pressure distribution for an ideal gas relative to the position in the column and takes the form (Perry et al., 1984):

$$\frac{P_0^2-P_z^2}{z} = \frac{2\sigma RT\mu G}{g_c M} + \left[\beta + \frac{1}{z}\ln\frac{P_0}{P_z}\right]\frac{2RTG^2}{g_c M} \qquad (2.20)$$

where:
- $P$ = absolute fluid pressure;
- $\sigma$ = empirical viscous resistance coefficient;
- $R$ = the universal gas constant:
- $T$ = absolute temperature;
- $\mu$ = the absolute viscosity of the fluid;
- $G$ = superficial mass velocity;
- $\beta$ = empirical inertial resistance coefficient;
- $g_c$ = gravitational dimensional constant;
- $M$ = molecular weight of fluid.

Equations 2.17-2.20, the Ideal Gas Law, and the sum of the porosities constitute the six equations necessary to fully describe the soil venting process in a one-dimensional laboratory column. The use of deep beds within such columns for the study of mass transfer parameters is mathematically complex. Because the governing system of equations can not readily be solved analytically, the system would require discretization and approximation. The remedy to such a complication is

the use of beds sufficiently thin so as to allow consideration of the bed as a differential element, thus, greatly minimizing the necessity for consideration of spatial variability within the column. Average values of pressure, porosity, interstitial velocity, and concentration may be employed to greatly simplify the mathematics while minimally compromising conformance with the true system. Experiments conducted using such systems can then concentrate upon the operative phenomena at the vapor/liquid interface rather than upon satisfying the mathematical structure of a fairly complicated system. Additionally, experimental runs would require time periods on the order of hours rather than days to complete. Experiments employing this technique are described in more detail in subsequent sections of this document.

# CHAPTER 3

# EXPERIMENTAL PROGRAM

## 3.1 OVERVIEW

The experimental program employed one-dimensional glass columns packed with thin beds of various grades of silica sand. Particle size distributions and particle shapes were determined experimentally. The soil beds were saturated with a pure-component NAPL (heptane) and drained to field capacity. Ultra pure air was then passed through the column at a constant molar flow rate. Gas flow was monitored upstream of the soil beds. Off-gas was assayed using gas chromatography with sample introduction consisting of a gas sampling valve and loop. Standard curves were prepared using liquid injections. A comparison was made between the responses per unit mass for liquid and gas injections. System pressure was monitored using transducers both upstream and downstream from the soil beds, upstream from a flow measurement device, and upstream from the sampling loop. Ambient pressure was measured before and after each experimental run. Output was recorded in a computer file via a data acquisition system for use in experimental analysis. A mass balance was closed upon the system for each experiment.

## 3.2 APPARATUS

### 3.2.1 Soil Column

A schematic of the differential column employed is shown in Figure 3.1. A schematic of the overall experimental system is shown in Figure 3.2. The column was custom designed and machined. The inlet and outlet manifolds and the perforated plates were fabricated from

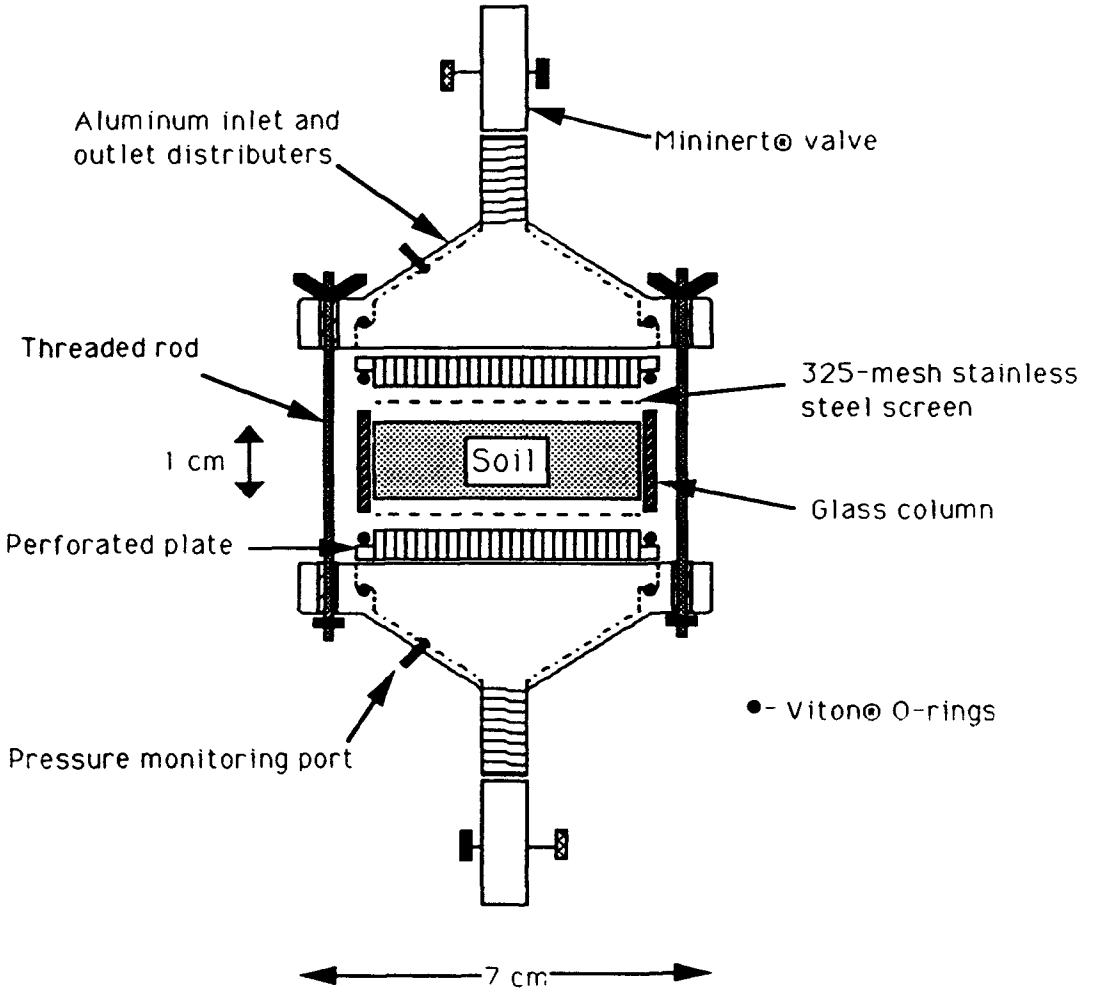


Figure 3.1: Soil column schematic.

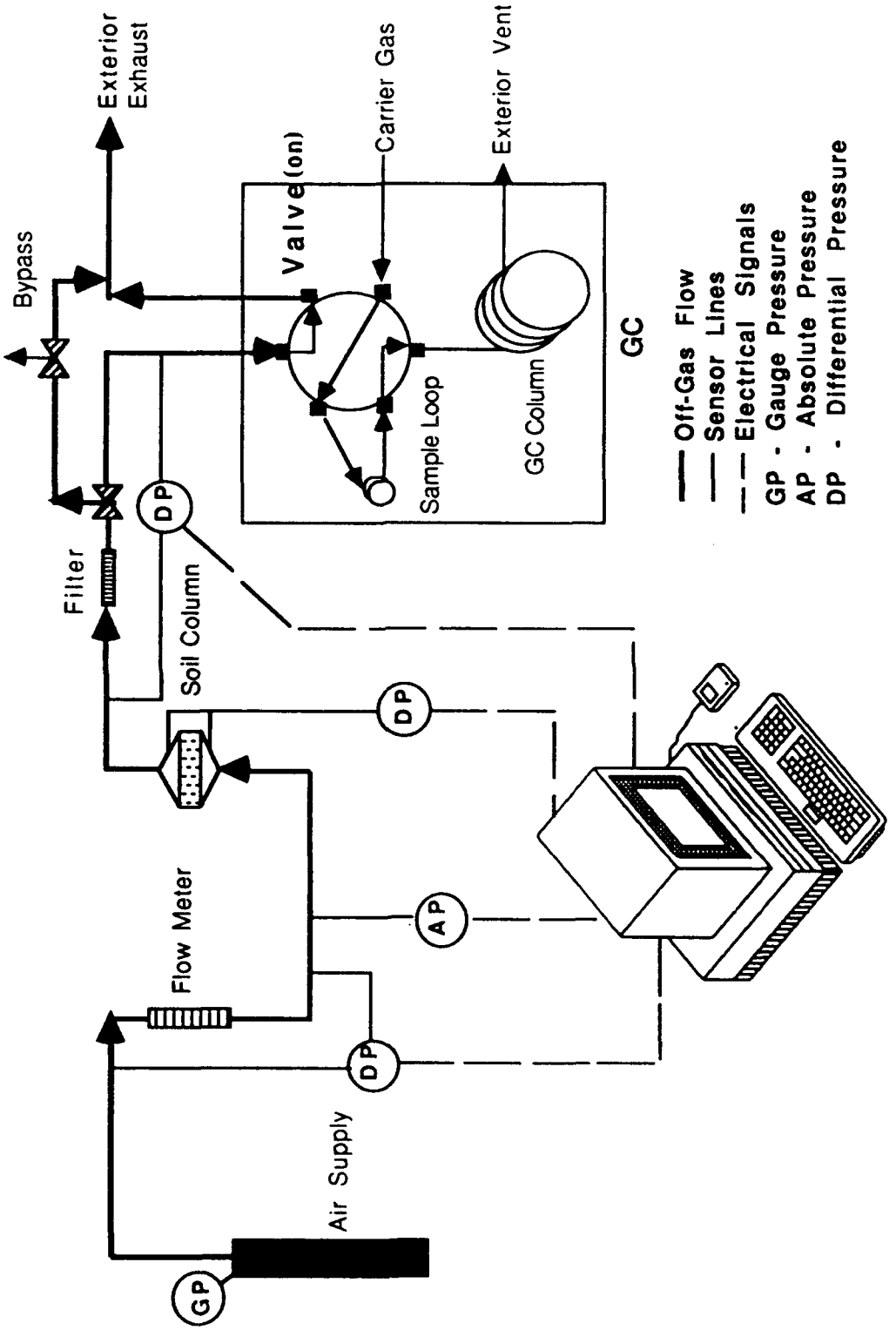


Figure 3.2: System schematic.

aluminum. An annular space, in combination with the perforated plate, provided for even loading of air over the area of the soil bed. The inlet and outlet manifolds each have an adapter for 1/8" tubing placed through the side wall to allow for connection of the differential pressure transducers. The soil bed was supported in the column using the perforated plates and 325-mesh stainless steel screens as a sandwich type containment system. The manifolds were compressed on to a medium-walled glass column (53 mm ID; 57 mm OD, 1 cm long) by six brass screws (1/8" X 1 1/4") and wing nuts. Viton® O-rings were used on either side of the brass plate to provide a gas-tight seal at the glass tubing/plate and the manifold/plate contact surfaces. Mininert® valves were used to connect the soil column inlet and outlet ports to a stainless steel compression fitting adapter. This adapter was then used to connect the column to the remainder of the system which consisted primarily of 1/4" O.D. copper tubing.

3.2.2 Gas Flow and Pressure Measurement

The gas flow rate was measured using a Fischer and Porter Purgemaster® 1/8" glass ball rotameter (model 10A6133MA1CXXXX3C1BC). The rotameter was factory calibrated and the calibration was verified as part of this effort. Details regarding the calibration performed are contained in Section 3.7.

Pressure transducers (absolute and differential) were located at various locations in the system. Absolute pressure was measured just prior to the column inlet using an Omega pressure transducer (model PX176-025A5V). Four Motorola differential transducers (model MPX5100-D/D) were used to determine the system pressures at the flowmeter

inlet, at the upstream and downstream sides of the soil bed, and near the inlet of the gas sampling loop. Knowledge of the pressure at these specific locations was necessary for calculation of volumetric flow rates, the mole fraction of heptane in the off-gas at saturation, and the molar quantity of gas residing in the gas sampling loop at the time of sampling. These calculations will be discussed in a later section.

The Omega absolute pressure transducer (0 - 25 psia) was factory calibrated and verified by a local precision measurements laboratory. The Motorola differential transducers were factory calibrated to have a very linear voltage response over the entire pressure range (0 to 15 psi differential). Each transducer calibration was verified by applying known differential pressures to the transducer and measuring the voltage. Calibration curves were used in the data acquisition process to convert voltage readings to pressure measurements. Constant power (+12 Volts) was supplied to the absolute transducer using an Elenco Precision power supply (model XP-580). Power (+5 Volts) was provided to the differential transducers by the Data Acquisition System (DAS). The DAS was a Keithley Metrabyte DAS-16 acquisition card compatible with IBM PC AT/XT type computers. The DAS was interfaced with the PC using Labtech Notebook® software version 6.0.1.

3.2.3 Sampling System

A pneumatically actuated switching system controlled through the Instrument Network (INET) system of the gas chromatograph was used to alternately route the off-gas from the experimental column through a sampling loop for injection into the gas chromatograph for assay. A Hewlett-Packard 5890 series II gas chromatograph equipped with a flame

ionization detector (FID), model 7673A automated liquid sampler, model 3396A electronic integrator, and split/splitless capillary injection was used for assay of the vapor phase.

The soil column off-gas passed through a 7 micron filter, to prevent solids from entering the GC, then through a 250 microliter Hewlett-Packard gas sampling loop located within an insulated controlled heated zone. A 2-way six-port valve was electronically and pneumatically controlled by the GC using inputs entered by the user at the GC keyboard. In the OFF position the soil column effluent passed through the loop and directly to an exterior vent. In the ON position the sampling loop was flushed by the carrier gas (He) and routed to the injector of the GC. The time required for flushing the sample from the sample loop was short, but sufficient time was given to ensure the sample was completely removed. The flushing time for the experiments was set at the GC for 0.3 minutes.

The plumbing for the sample loop system consists of 1/16" stainless steel tubing. This resulted in excessive pressure losses through the system when the entire flow of off-gas was passed through the sample loop. A bypass system was therefore installed to route a majority of the effluent directly to the exterior vent, while passing a portion through the sampling loop. Pressure drop through the sampling loop was then minimized. Valving was installed in the bypass lines to control the split and to aid in measuring flows as necessary.

## 3.3 MATERIALS

### 3.3.1 Pure-Component NAPL

Typical operations which are commonly found to be sources of vadose zone contamination by VOCs were considered in selecting a target solute. Jet fuel (JP-4) is clearly the most common VOC mixture used by the Air Force. Large quantities of fuel are stored in underground tanks and transferred to aircraft; thus, many sites at Air Force facilities have been contaminated by jet fuel. Because the composition of JP-4 is extremely complex, use of the fuel itself would unduly complicate analysis of the experiments. One prevalent component of JP-4 is n-heptane. This solute represents a rather volatile component of JP-4. Gasoline leaks/spills are also prevalent at Air Force Installation Restoration Program (IRP) Sites. N-heptane is also an important component of gasoline. Therefore, heptane was chosen as the initial experimental component. The n-heptane used was obtained from the Aldrich Chemical Company, catalogue number 27,051-2. Its purity exceeded 99.6%.

### 3.3.2 Soils

The soils investigated in this study were medium to fine silica sands of known composition and character. These silica sands (grades 2, 3, and 6 ) were supplied by the Agsco Corporation of Wheeling, Illinois. Two silica flour samples were also obtained from Agsco. One sample was retained on a #200 sieve and the other retained on a #325 sieve. Attempts were made to use these soils in the experimental column. Unfortunately, excessively high pressure losses were associated with relatively low air flows; thus, these soils were not

used in this investigation. Additional study of pressure loss as a function of air flow and particle size is warranted in order to identify a limiting particle size for soil venting. The grain size analyses provided by the manufacturer for the grades used are shown in Table 3.1.

Table 3.1

**U.S. Standard Sieve Analyses of Silica Sand Samples**

| MESH SIZE | GRADES 2 | 3 | 6 |
|---|---|---|---|
| | Percent Retained on Sieve | | |
| 20 | 2 | | |
| 30 | 32 | T | |
| 40 | 55.3 | 29 | 2 |
| 50 | 10.2 | 41 | 24 |
| 60 | 0.5 | | |
| 70 | | 23 | 34.5 |
| 100 | | 6 | 28.5 |
| 120 | | 1 | |
| 140 | | | 8 |
| 200 | | | 3 |

T - trace

Sieve analyses were performed for each of these samples as part of this investigation to verify the data of the supplier. In some instances, the grain size distributions obtained did not agree with those of the supplier (differences of 10% were noted). To be confident of the grain size distribution of the soils used in the experimental columns, careful sieving of these samples was necessary.

### 3.3.2.1 Separation of the Distinct Grain Sizes for the Soil Column Materials

Three poorly-graded soils were assembled by dry sieving these silica sands. These three soils had grain size distributions such that 100% of the material passed the 30, 50, and 80 sieves and 100% was retained on the 40, 60, and 100 sieves, respectively. U.S. Standard 3-inch sieves conforming to ASTM E-11 specifications were used. Samples were mechanically shaken for no more than 15 minutes. The respective size fractions were collected for use in packing the soil columns.

### 3.3.2.2 Sphericity Measurements

Portions of the three samples were placed on a slide and prepared for Phase Contrast Microscopy analysis. Two-dimensional measurements were made under the microscope of at least 50 randomly chosen particles of each soil. The long and short dimension were recorded for each particle. A program written for an HP28S calculator (Davis, 1991) was then used to statistically determine the shape factor (sphericity) for the three samples. The shape factor is defined as the ratio of the exterior surface area of the particle to that of a sphere of an equivalent volume. The particles were assumed to be prolate spheroids with a thickness equal to the measured short dimension of the particle for these sphericity calculations. The resulting sphericity estimations (listed in Table 3.2) were all very close to unity which is as expected for silica sand.

### 3.3.2.3 Physical Characteristics of the Soil Samples

The physical parameters of the three soil samples were determined as discussed previously and are listed in Table 3.2. The specific surface area of the solid particles, $\alpha_p$, was estimated as that of a

sphere of equivalent volume such that $\alpha_p$=6/d. The solid surface area of the whole soil was estimated by assuming a random packing arrangement of spherical particles. The diameter used in computations of $\alpha_p$ for each

Table 3.2

Physical Parameters for Silica Sand Samples

| Parameter | Bed Size 30/40 | 50/60 | 80/100 |
|---|---|---|---|
| Largest diameter, mm | 0.60 | 0.30 | 0.18 |
| Smallest diameter, mm | 0.425 | 0.25 | 0.15 |
| $d_{10}$, mm | 0.440 | 0.255 | 0.153 |
| Sphericity | 1.022 | 1.023 | 1.017 |
| $\alpha_p$, $cm^2/cm^3$ | 136 | 235 | 393 |

whole soil was the $d_{10}$, the diameter that 10% of the material in a mixture is finer. The $d_{10}$ is often referred to as the effective size of a soil mixture. The $d_{10}$ of each soil was obtained from a log-linear interpolation from the respective two-point grain size distribution.

## 3.4 EXPERIMENTAL MATRIX

Five target air flow rates were employed with each soil bed as measured by the ball travel in the rotameter: 15 mm, 40 mm, 70 mm, 110 mm, and 140 mm These values of float travel roughly correspond to interstitial velocities in the experimental beds that are within the range encountered in soil venting systems. Experimental runs were replicated at a rate of 20% of the total number of runs with random selection of the replicates. Additionally, runs were repeated when the

mass balance closure did not fall within one standard deviation of the mean closure error, as will be discussed in a later section.

## 3.5 EXPERIMENTAL PROCEDURES

Significant preparation was necessary prior to initiation of experimental runs. These preparations included packing the soil column, loading the soil column with the heptane, optimizing the analytical system, and calibrating the analytical system.

Ultra-pure carrier (UPC) air was used as the convective phase and flow rates were set at the values discussed previously. The off-gas concentration was measured as frequently as possible using the GC. A maximum rate of one sample every two minutes could be attained. GC operating conditions were optimized to provide for separation of heptane from methanol for standard curves using the minimum possible run time.

### 3.5.1 Packing the Soil Column

An adhesive (Loctite Corp., Duro® Depend II), resistant to both water and petroleum products, was used to attach the 325 mesh stainless steel screen to the aluminum diffuser plate. Small quantities of the adhesive were dabbed on to the periphery of the plate to secure the screen flat on the plate. This adhesion was critical to prevent migration of sand past the screen and subsequent loss from the column. The adhesive was oven-dried for at least four hours for curing.

The column was weighed on a Sartorius balance (+/- 0.01g) with all of the parts necessary to pack the column (glass, O-rings, plates, bolts, and wing-nuts). The bottom half of the column (consisting of one manifold, two o-rings, the diffuser plate with attached screen, and

glass) was placed in a ring stand. The soil was placed in the column using water consolidation to simulate natural conditions as closely as possible. The sand was added in small amounts, spread evenly, then saturated with distilled water. A light vacuum was then applied to the lower connection of the column to draw off the excess water. This procedure was repeated until the level of sand was just below the top of the glass column. The lower face of the upper diffuser plate extends below the upper level of the glass column. Sand was then added as necessary to fill any detectable voids. Sand was then removed from the top of the glass, from the O-ring, and from the O-ring groove on the diffuser plate prior to final sealing. This ensured an air-tight seal. The six bolts and wing nuts were then fastened to the column and tightened sufficiently by hand to maintain all components in place. The column was then given a final water rinse to remove remaining loose sand, and oven-dried at 60°C. The drying process continued until a constant mass was obtained for three consecutive weighings (at least overnight). Absolutely dry conditions were critical for these soil venting experiments which involved only a single component organic phase. The presence of moisture would have introduced another phase, constituting two additional equilibrium conditions and two additional interfaces for mass transfer. Undesirable complexity would be associated with the physical system severely compromising the capability to determine gas-side mass transfer coefficients.

Volumetric measurement of the empty column and known solid particle density ($\rho_s$ = 2.65 g/cm$^3$) values then allowed the calculation of the total void fraction, $\epsilon_t$. Three identical columns were packed

with the three grades of silica sand and used for all experiments without disturbance. In this manner, the behavior of the system in response to the targeted experimental conditions could be evaluated independently of differences in the bed.

3.5.2 Soil Column Preparation

Loading of the soil bed with the heptane was accomplished using slight vacuum aspiration, as described by Marley and Hoag (1984). Initially, the amount added was sufficient to completely saturate the bed as observed through the glass column. Initial experiments showed that complete saturation was not necessary, because a steady removal rate was observed for some time after the start of a run. Subsequently, air was used to remove some of the heptane to render the initial column loading below field saturation. The initial mass of heptane present was measured by weighing the column and attachments both before and after the addition of the heptane. The difference of the two weighings constituted the initial mass added. The volume fraction of the liquid phase, $\epsilon_l$, was then computed from the mass and density of the heptane. The volume fraction of the vapor phase , $\epsilon_v$, was computed as the difference between $\epsilon_t$ and $\epsilon_l$.

3.5.3 Calibration of Rotameter

A variable area flowmeter was used for measuring the air flow rate as discussed in Section 3.2.2. The meter was supplied with a +/- 1% calibration curve of float travel (millimeters) versus flow rate in Standard Cubic Feet per Hour (SCFH) metered at an absolute pressure of 1 atmosphere and 25$^{o}$C. A standard cubic foot was defined by Fischer

and Porter at a pressure of 1 atmosphere absolute and a temperature of $70^{o}F$.

A laboratory calibration of the rotameter was performed as part of this investigation. Actual flow rates were measured at various float travel readings using the water displacement method to verify this calibration. A 2-liter Erlenmeyer flask was calibrated to a mark by adding a known mass (+/- 0.01 g) of water, allowing it to come to room temperature, and determining the volume by dividing the mass by the density of water at that temperature. This flask was then filled with water at room temperature and inverted into a five-gallon plastic bucket filled with water. While under the water, the flask was capped with a two-hole rubber stopper, which had been fitted with glass tubing through one of the holes. The glass tubing was shaped so it could be easily attached to the downstream side of the meter via flexible tygon tubing and 1/4" O.D. copper tubing. This tubing had been previously filled with water to evacuate any air. The time necessary to evacuate the water in the flask down to the mark was measured at various distances of float travel. The level of the water in the flask was always kept at the same level as the water outside the flask to avoid necessitating corrections due to water level differences between the interior and exterior of the flask. Pressure measurements were made using the absolute and differential pressure transducers to record the system pressures during the calibration. Room temperature was also measured and recorded. These temperature and pressure measurements were then used to convert the measured flow rates to standard cubic

feet per hour at 1 atmosphere and 70°F. The calibration was within +/- 3% of the factory calibration.

3.5.4 Mass Transfer Experiments

A loaded soil column was connected to the system with the Mininert® valves in the closed position. A two-stage regulator valve was opened at the UPC air tank to provide a constant air supply pressure. A leak check was performed on the entire system by pressurizing isolated sections of the flowpath. If any leaks were present, it was indicated by a small float travel in the rotameter, then the location was isolated using a soap film technique. First, with the Mininert® valves closed, the system prior to the soil column was checked. Next, the upstream Mininert® valve was opened and the soil column was checked for any leaks. To check downstream from the soil column, the downstream Mininert® valve was opened and the valving in the bypass loop was closed. This last check was only done periodically since these connections were not altered as often as the others. For this check, an empty soil column was used since the use of a loaded soil column would have removed some heptane from the soil affecting the mass balance.

The liquid standards were assayed prior to each run. The GC was then setup for gas sampling by programming the gas sampling valve operation into the GC control panel. The DAS program was then recalled by the computer. Time settings on the computer, the HP integrator, and a personal watch were synchronized. To begin a run, the Mininert® valves were opened, while at he same time the DAS program was started. The rotameter setting was quickly adjusted to the desired flowrate.

After one minute, the first sample was assayed. The retention time for heptane was appoximately two minutes. Therefore, the maximum sample frequency was slightly greater than two minutes. During periods of a steady FID signal, samples were taken every 6 to 10 minutes. For rapidly changing periods, samples were taken as frequently as possible.

When detection peak areas became very small (less than approximately 100 millivolt-seconds), the sampling was stopped by closing the Mininert® valves, stopping the DAS, and closing the air supply valve. The soil column was disconnected from the system and weighed.

The soil beds were made relatively thin, so experimental runs were complete within one half to a few hours. The semi-automated gas sampling of column off-gas allowed an optimal number of data points to be accurately generated during each run.

Post-calibration of the GC was perfomed by repeating the liquid standard injections after each run.

## 3.6 ANALYTICAL METHODS

### 3.6.1 Assay of Column Off Gas

The chromatographic column used was a 25m X 0.31mm I.D. fused silica capillary column with a stationary phase consisting of a 0.52 micron, crosslinked, 5% phenyl methyl silicone film. This column was manufactured by Hewlett-Packard and was model HP-1.

A carrier solvent was necessary for the standards used for calibration using liquid injection. Methanol was chosen since its retention time in the GC column was relatively short, and the corresponding peak could be easily separated from the heptane peak.

Four standards (7.372 mg/l, 71.67 mg/l, 764.4 mg/l, and 65.77 g/l) of heptane in methanol were independently prepared and chilled to 4°C for future use. The GC was operated in the split mode with a split ratio of approximately 10:1. The oven temperature was set at 65°C and the analyses were performed isothermally. Carrier gas flow was approximately 28-30 ml/min with a column head pressure of 12.5 psi. The resulting residence times were about 1.1 and 1.9 minutes for methanol and heptane, respectively. A hard copy output of each run included a pictorial chromatogram, measured run time, and integrated peak areas.

3.6.2 GC Standard Preparation

Liquid standards were made by gravimetrically adding heptane to a known quantity of methanol. An 80 ml glass vial fitted with a two-piece Teflon®-lined closure was weighed empty (+/- 0.0001 g), filled with methanol, and then reweighed to determine the mass of methanol added. The density of methanol at room temperature was used to determine the volume of methanol in the vial. Hamilton gas-tight syringes of different sizes were used to add n-heptane to the methanol. The syringe was weighed (+/-0.0001 g) before and after the addition to determine the mass added. A mass per unit volume concentration was then calculated. The quantity of heptane added for three standards was sufficiently small and, thus, was negligible in computation of the total volume of the standard. One out of the four standards prepared had an appreciable amount of heptane added (65.77 g/l). In this case zero volume change was assumed and the two volumes (methanol and heptane) were added to obtain the total volume. Though perfect mixing

probably did not occur, this difference should not cause more than a 1-2% error in the actual concentration of the standard. This error is most likely overshadowed by the repeatability of the GC at the high concentration of this standard.

3.6.3 Calculation of the Heptane Concentration

A calibration curve of the Flame Ionization Detector (FID) response in millivolt-seconds (mv-sec) versus the standard mass injected (milligram per one microliter injected) was obtained for each experimental run. The regression formula used was:

$$y = mx \tag{3.1}$$

where: y = ordinate (response, mv-sec);
x = abscissa (standard mass, mg); and,
m = the slope of the curve ($\Sigma xy/\Sigma x^2$).

Each of the four standards were introduced into the GC using automatic liquid injection of a 1 microliter sample. Calibration curves were obtained both before and after each run to detect altered instrument conditions or signal drift over the course of a run. A regression was obtained for both sets of data and a value of m obtained. Coefficients of determination ($R^2$) for the curves were always greater than 0.999. A percent change between the two slopes was calculated and, as may observed from Table 3.3, were within the range of +/- 5%. Each set of pre- and post-run calibrations were then combined into a single regression for computation of the unknown off-gas concentrations from gas sample responses. The detector response for each gas sample taken during an experimental run, was divided by the slope of the overall calibration curve to obtain the mass of heptane residing in the gas sampling loop.

Table 3.3

Liquid Standard Calibration Parameters

| Run #/Flow Reading(mm) | Pre-Run Slope(m)[a] | Post-Run Slope(m)[a] | % Change | Combined Slope(m)[a] | $R^2$ |
|---|---|---|---|---|---|
| 30-40 Mesh | | | | | |
| 26 / 15 | 3.161 | 3.092 | -2.18 | 3.127 | .9998 |
| 51 / 40 | 3.484 | 3.341 | -4.11 | 3.412 | .9993 |
| 49 / 70 | 3.440 | 3.523 | +2.43 | 3.482 | .9998 |
| 56 / 70 | 3.265 | 3.095 | -5.21 | 3.180 | .9990 |
| 48 / 110 | 3.364 | 3.442 | +2.32 | 3.403 | .9998 |
| 47 / 140 | 3.330 | 3.380 | +1.52 | 3.355 | .9999 |
| 50/60 Mesh | | | | | |
| 61 / 15 | 3.593 | 3.628 | +0.98 | 3.610 | 1.0 |
| 71 / 15 | 3.486 | 3.390 | -2.75 | 3.438 | .9997 |
| 57 / 40 | 3.380 | 3.531 | +4.47 | 3.456 | .9992 |
| 58 / 70 | 3.531 | 3.579 | +1.35 | 3.555 | .9999 |
| 59 / 110 | 3.611 | 3.696 | +2.35 | 3.653 | .9998 |
| 69 / 110 | 3.210 | 3.324 | +3.52 | 3.267 | .9996 |
| 70 / 110 | 3.324 | 3.266 | -1.73 | 3.295 | .9999 |
| 72 / 110 | 3.096 | 3.082 | -0.43 | 3.089 | .9999 |
| 60 / 140 | 3.696 | 3.593 | -2.80 | 3.644 | .9997 |
| 80/100 Mesh | | | | | |
| 63 / 15 | 3.641 | 3.608 | -0.91 | 3.625 | .9999 |
| 64 / 40 | 3.608 | 3.491 | -3.24 | 3.546 | .9995 |
| 65 / 70 | 3.624 | 3.657 | +0.92 | 3.641 | .9999 |
| 66 / 110 | 3.657 | 3.536 | -3.31 | 3.597 | .9995 |
| 67 / 140 | 3.536 | 3.537 | +0.02 | 3.537 | .9999 |

[a] - Units are $10^8$ millivolt-seconds/mg. Regression slopes for the pre and post run calibrations all had correlation coefficients greater than 0.9999.

### 3.6.4 Determination of the Mole Fraction of Heptane

The molar quantity of heptane in each 250 $\mu$l sample was obtained from the mass detected by division by the molecular weight of heptane (100.2 g/gmole). The molar quantity of vapor in the gas sampling loop was obtained by assuming the ideal gas law to be valid such that:

$$n_v = PV/RT \qquad (3.2)$$

where: $n_v$ = the moles of vapor in the sampling loop;
P = the pressure of the sampling loop (atm);
V = the volume of the sampling loop (250 X $10^{-6}$ l);
R = universal gas constant (0.082057 l-atm/gmole-$^{o}$K); and,
T = the temperature of the sampling loop (388 $^{o}$K).

The temperature of the insulated area in which the sampling loop resides was set at 115$^{o}$C. Heat transfer calculations were performed on the system to verify that the off-gas would be at this temperature as it entered the sampling loop. Results of these calculations showed that the off-gas easily achieved this temperature.

Observed pressure drops across the sampling system during an experiment were consistantly 0.2 to 0.4 tenths of a psi. Connections and tubing on the upstream and downstream sides of the sampling loop were identical so the system was assumed to be symmetrical around the gas sampling loop. The pressure of the loop was therefore closely estimated by determining the average of the inlet and outlet (ambient) pressures.

### 3.6.5 Closure of the Mass Balance

A mass balance was performed for each mass transfer experimental run to correlate the off-gas analyses with the quantity of heptane actually removed from the soil column. The molar flow rate of heptane in the column off-gas was calculated using the results of off-gas assay

in combination with the measured rate of air flow to the system such that:

$$m_h = m_a(1 + Y_h)Y_h \qquad (3.3)$$

where: $m_h$ = molar flow rate of heptane;
$m_a$ = molar flow rate of air applied; and,
$Y_h$ = mole-fraction concentration of heptane in the off-gas.

The molar flow rate of heptane was plotted against time and total mass removed was then calculated by integrating the resulting relationship over the elapsed time of the experiment using a trapezoidal approximation. The results of these computations were then compared to the actual gravimetric changes in column mass for each run.

As will be discussed in more detail in Section 4.2, the mass balance did not close. It was determined that a mass-specific response for liquid and gas injections were different. An attempt was made to determine the magnitude of this difference by volatilizing pure pentane through the gas sampling loop and comparison of these FID responses to responses from liquid pentane injections.

# CHAPTER 4

# RESULTS AND DISCUSSION

## 4.1 PROFILES OF OFF-GAS CONCENTRATION VERSUS TIME

Off-gas concentration was plotted for each experimental run as a function of time and these plots are presented as Appendix A. From the off-gas concentration profiles it can be observed that at least two distinct regions exist. The profiles for the lower air flow rates have a third distinct region which occurs at early times. This region, Region 1, is characterized by increasing heptane concentrations at early run times. Region 2, the flat portion of the profiles, is characterized by a relatively constant heptane concentration in the off-gas over various lengths of time depending on the air flow rate. Region 3 is characterized by a decreasing heptane concentration. Region 1 is not observed at higher flow rates. Apparently, the conditions resulting in this region of the profile disappear before GC sampling can be accomplished under conditions of high air flow.

## 4.2 CLOSURE OF MASS BALANCES

The area under each off-gas concentration versus time curve represents the total mass of heptane removed from each soil column and should correlate with the gravimetrically measured heptane removal. As discussed previously the area under each of these profiles was integrated to obtain a computed value of the quantity of heptane removed. The results of these computations are listed in Table 4.1. The percent recovery, taken as the computed mass removed divided by the gravimetrically measured mass removed is plotted versus rotameter setting in Figure 4.1.

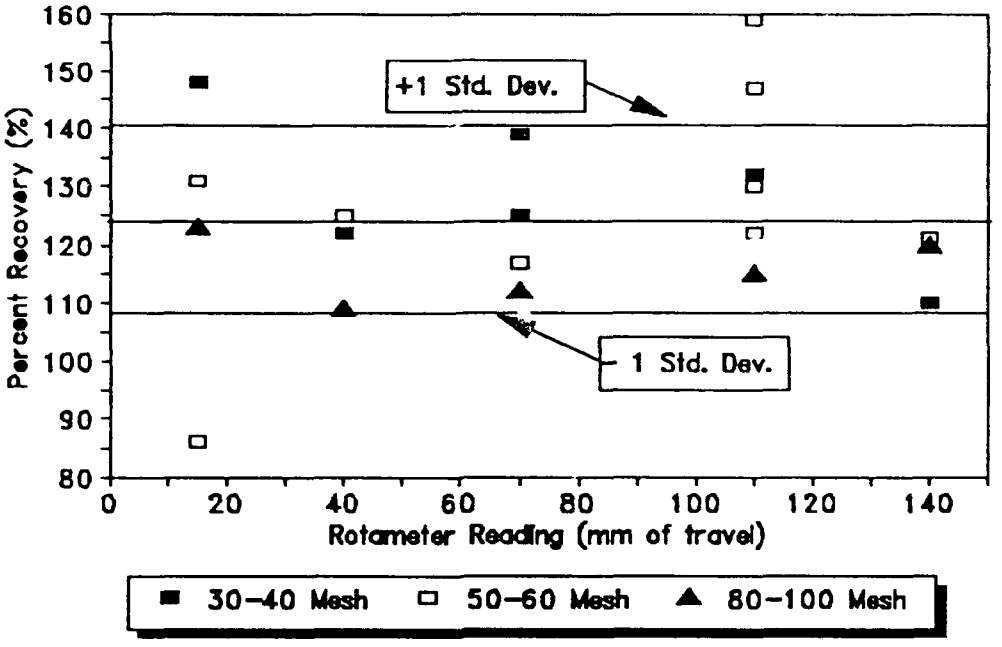


Figure 4.1: Computed percent recovery of heptane at various flow rates for the three different soil columns.

The average percent recovery was 124.6% with a standard deviation of 16.1%. As may be observed from the Figure 4.1, the recovery percentage does not appear to be related to flow in any way. The errors in the mass balance appears to be both a random and systematic, probably associated with the analyses of off-gas concentrations. Variations in the response of the detector to a given mass of heptane introduced as a liquid versus a vapor were considered as a possible explanation. N-pentane was heated to its boiling point in a closed system with the generated vapor allowed to flow through the gas sampling loop. Pentane was used as the experiment could be accomplished without supplemental heating of transfer lines to prevent condensation. Such an experiment for heptane (boiling point - 98$^{o}$C) would necessitate such a system. Pentane has a structure and

properties similar to those of heptane; thus, behavior in this experiment should be similar to that of heptane. The system was flushed for a period of time after the pentane began to boil to allow evacuation of air from the lines prior to sampling. Samples of this stream were analyzed using the gas sampling loop until the response of the FID came to a constant value. The operating conditions of the GC and sampling loop were set to correspond with those of the experimental runs involving heptane. The number of moles of pentane present in the sampling loop at the temperature and pressure of the loop was computed using the Ideal Gas Law. Liquid injections of n-pentane were done repeatedly before and after the gas sampling. The corresponding responses indicated that the operating conditions of the GC did not drift over the course of the run. A comparison was made between the liquid mass injected and the calculated mass from the gas sampling. The ratio of the response per unit mass for the gas introduction was 126% of that for liquid introductions. The systematic error in the mass balance recovery, then, appears to be related to a yet undefined difference related to the method of sample introduction. Other compounds should be tested in this manner to conclusively determine whether this observation is specific only to the injection method or to both the introduction method and the specific compound in question. Based on evidence that liquid versus gas sample introduction results in a systematic difference, verification of the flow meter calibration as discussed in Section 3.6.1, and the gravimetric measurement of the actual quantity of heptane removed from each column, the experimental off-gas concentration versus time profiles were normalized to the actual quantity of heptane removed. This normalization was

accomplished by dividing the off-gas concentrations measured using chromatography by the recovery fraction. The plots shown in Appendix A reflect this normalization. The areas under these curves (moles heptane) therefore equate to the actual gravimetric changes in the mass of each soil column for each experimental run.

## 4.3 APPARENT OVERALL GAS-SIDE MASS TRANSFER COEFFICIENT ($k_v\alpha$)

The product of the mass transfer coefficient and the interfacial surface area ($k_v\alpha$) was determined using Equation 2.17 for each measurement taken during each experimental run. These values were plotted against the corresponding modified Reynolds number (Re'). All runs performed on each soil column were plotted on the same graph and labeled corresponding to the terminal pore velocity. The terminal pore velocity can be defined as the limiting value of the velocity of the convective air stream within the pores of the soil bed as the heptane is depleted to an insignificant amount of mass. The terminal pore velocity was used to identify each run since it is analogous to the superficial velocity divided by the dry bed porosity. This is specific to each bed and flow rate. These plots are shown in Figures 4.2 - 4.4.

The magnitude of Re' for each of these runs decreases as run time increases due to the removal of heptane from the pores. This corresponds with decreases in the pore velocity term of Re' associated with to increases in the effective pore diameter as the heptane is removed. This continues until a terminal pore velocity and a terminal effective pore diameter are reached. Two distinct regions are clearly visible on these plots. Three distinct regions can be observed from another plot that includes only those runs of low terminal pore velocity.

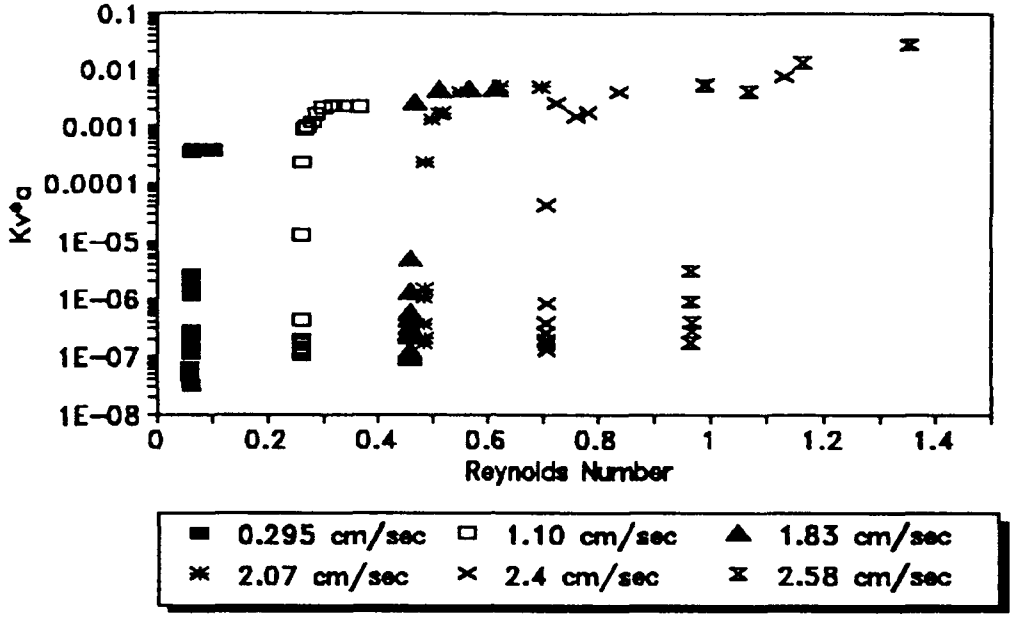


Figure 4.2: A plot of $k_v a$ (moles/$cm^3$-min-mole fraction) versus modified Reynolds number, Re', for 30/40 mesh soil and various average terminal pore velocities ($U_t$).

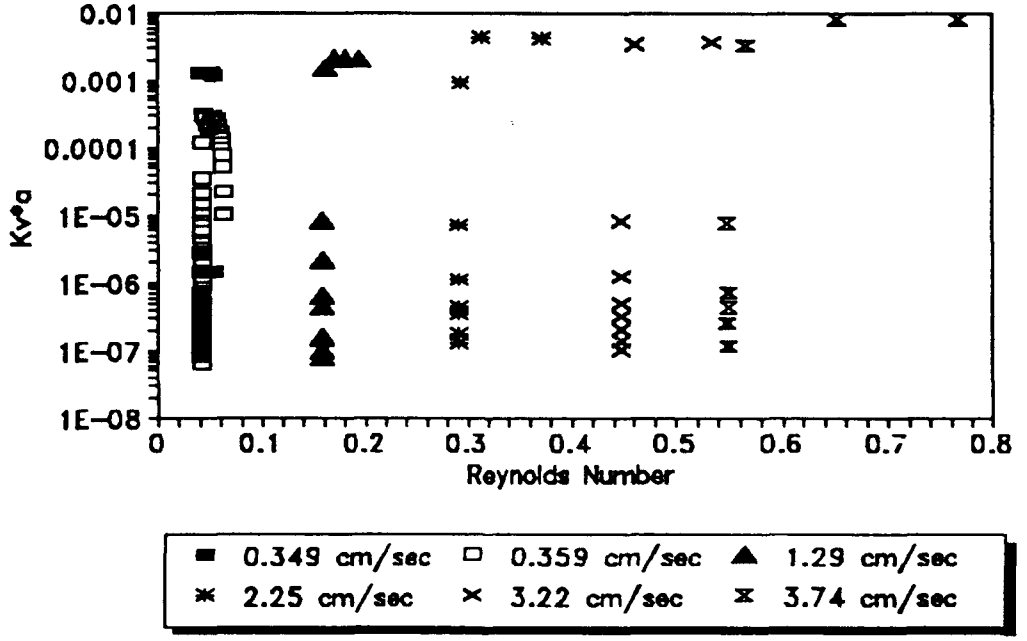


Figure 4.3: A plot of $k_v a$ (moles/$cm^3$-min-mole fraction) versus modified Reynolds number, Re', for 50/60 mesh soil and various average terminal pore velocities ($U_t$).

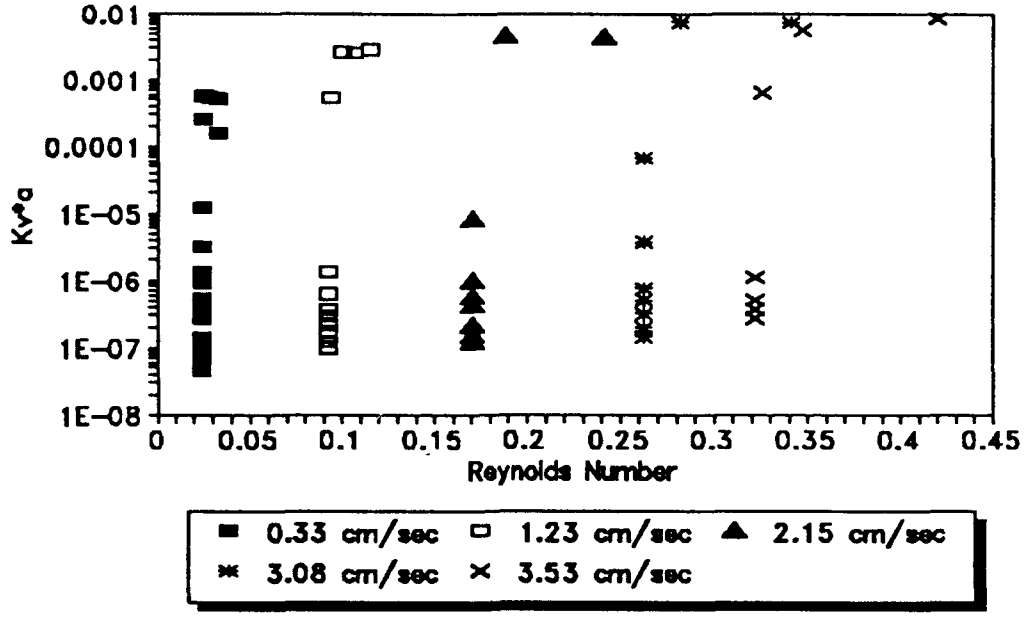


Figure 4.4: A plot of $k_v a$ (moles/cm$^3$-min-mole fraction) versus modified Reynolds number, Re', for 80/100 mesh soil and various average terminal pore velocities ($U_t$).

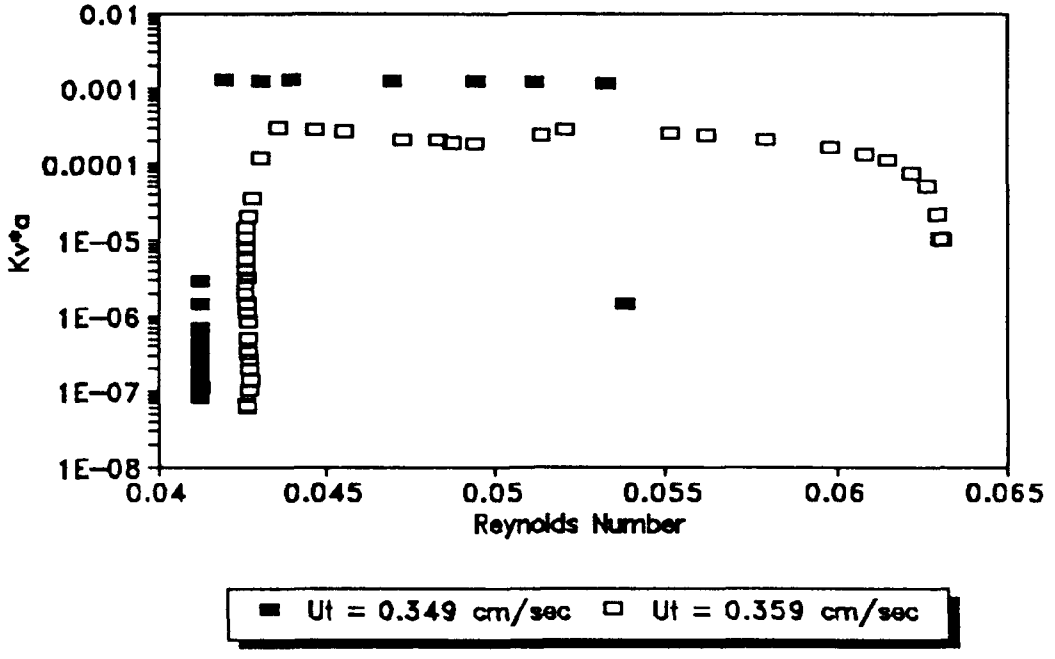


Figure 4.5: A plot of $k_v a$ (moles/cm$^3$-min-mole fraction) versus modified Reynolds number, Re', for low flow rates - 50/60 mesh soil column.

Two curves from Figure 4.3 ($U_t$ = 0.349 and 0.359 cm/sec) are replotted in Figure 4.5. In both runs, the value of $k_v\alpha$ increases initially to a fairly constant maximum and then decreases sharply at later run times beyond some threshold quantity of heptane remaining in the soil. The increasing $k_v\alpha$ (Region 1, the right side of the data plots in Figure 4.5) can be explained by a rising value of $\alpha$. Upon initiation of air flow through the column the pores in the soil may not be fully developed. When all potential void spaces in the soil are open to air flow, the pores are then fully developed. As heptane is removed, additional pores develop producing additional flow paths through the soil matrix and additional vapor/liquid interfacial surface area. The magnitude of $k_v$ may decrease slightly during this portion of the curve, since the distance across which mass transfer occurs becomes larger due to the corresponding increase in the effective pore diameter and the rapid decrease in the pore velocity. A corresponding increase in $\alpha$ obviously overshadows this decrease in $k_v$, resulting in a combined increase in $k_v\alpha$. This process continues until the pores are fully developed, resulting in the flat portion of the profile.

The regions of constant $k_v\alpha$ that may be observed in Figures 4.2-4.5 over significant ranges of Reynolds numbers are analogous to a constant drying period. Gamson et al. (1943) and Wilke and Hougen (1945) observed similar behavior during drying of porous ceramic spheres and cylinders. These experiments involved a single vapor/liquid interface situated at the surfaces of spherical and cylindrical particles, and particle sizes were much larger than those of this study. Additionally, since these particles were able to absorb water, a pore structure did exist within these particles. Rogers and

Kaviany (1990) also observed a period of constant drying that they termed as a "funicular drying p~riod". Their experiments involved the evaporation of water from beds of spherical glass particles (d < 3mm) by passing a stream of warm air over the beds. Constant rates of evaporation were observed over significant time periods. The constant drying period of Gamson et al. (1943), Wilke and Hougen (1945), and Rogers and Kaviany (1990) maybe explained by redistribution of the water in the pores to maintain a constant wetted area at the surface of the bed from which mass transfer occurred. A somewhat different situation was prevalent in the soil beds of this investigation. The packed bed of Rogers and Kaviany (1990) represents the passage of air over a porous planar surface of large pores, different from the ceramic materials of Gamson et al. (1943) and Wilke and Hougen (1945) only in the size of the pores.

Previous studies all indicate that the magnitude of the mass transfer coefficient, k, is directly related to a power of the Reynolds number. During the entire constant rate region Re' decreases. Correspondingly, this should result in a decrease in the mass transfer coefficient, $k_v$. Then, in order for $k_v\alpha$ to remain relatively constant as may be observed from Figures 4.2-4.5, $\alpha$ must then increase. During the portion of the experiments in which the volatilization rate is constant, heptane is present at all particle-particle contact points. The ramifications of these changes is not readily discernable. The interfacial surface area will depend on the size of the solid particles, the contact angle between the liquid and solid (specific to the composition of the NAPL), the quantity of the NAPL present and the temperature. As is discussed later, an analytical solution using

three-dimensional calculus and assuming spherical particles may be employed to estimate the magnitude of $\alpha$ on a NAPL-specific basis. The data represented in Figures 4.2-4.4 suggest that $k_v\alpha$ does decrease as Re' decreases at higher flow rates,. This may suggest that $\alpha$ is in fact constant over this range or changes very little.

A condition is reached during these experiments such that the rate of mass removal begins to decrease rapidly. Removal of heptane beyond this condition results in the behavior observed in Region 3. Region 3 of Figures 4.2-4.5 is characterized by a rapidly decreasing magnitude of $k_v\alpha$ at relatively constant Reynolds numbers. Relationships between $k_v\alpha$ and the mass of heptane remaining in the column for data falling within Region 3 are shown in Figures 4.6-4.9. As the mass remaining in the bed decreases so does $k_v\alpha$. The magnitude of Re' is constant throughout this region due to small changes in the pore velocity and the effective pore diameter. Consequently, the characterization of the behavior in this region for the various soils is in terms of the terminal value of the modified Reynolds number, $Re'_t$, computed based on the experimental air flow rate and the bed devoid of heptane. During this region of behavior, the magnitude of $\alpha$ decreases rapidly due to depletion of heptane from the pores. Moreover, the magnitude of $k_v$ may also decrease significantly. Some particle-particle contact points become devoid of heptane. therefore the transport distance to the air stream is greater. Perfect mixing can be assumed in each pore, but not between adjacent pores. The observed values of $k_v$ may decrease as a ramification of

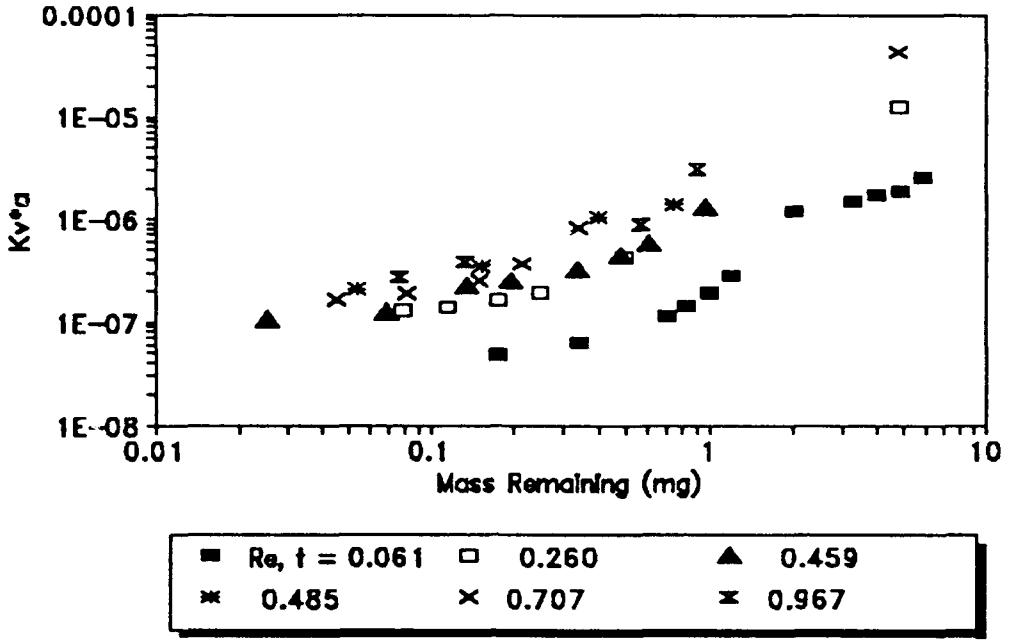


Figure 4.6: A plot of $k_v a$ (moles/cm$^3$-min-mole fraction) versus the mass of heptane remaining in the 30-50 mesh soil column for various terminal modified Reynolds numbers, $Re'_t$.

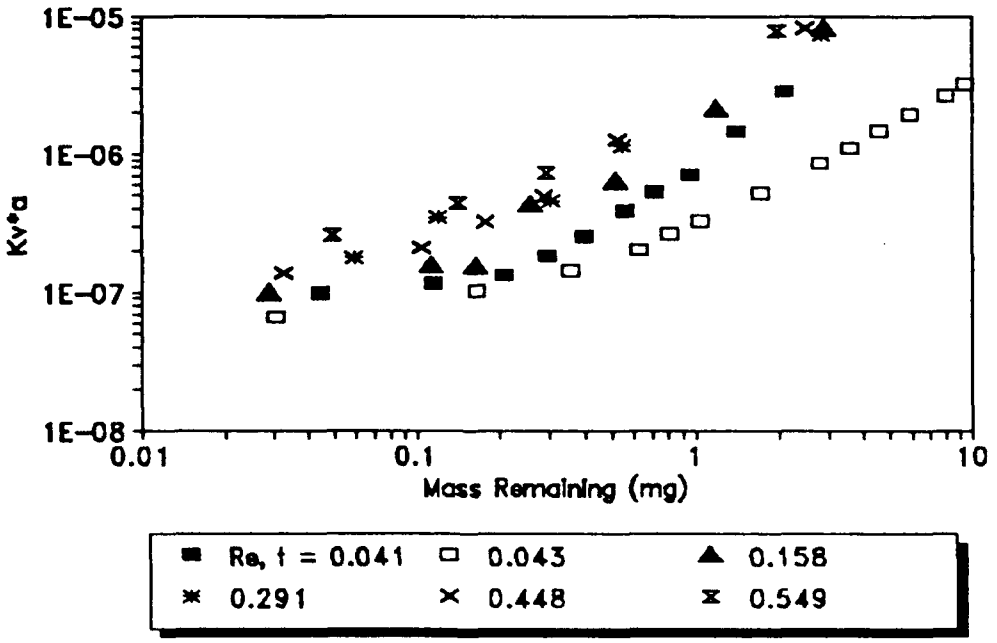


Figure 4.7: A plot of $k_v a$ (moles/cm$^3$-min-mole fraction) versus the mass of heptane remaining in the 50-60 mesh soil column for various terminal modified Reynolds numbers, $Re'_t$.

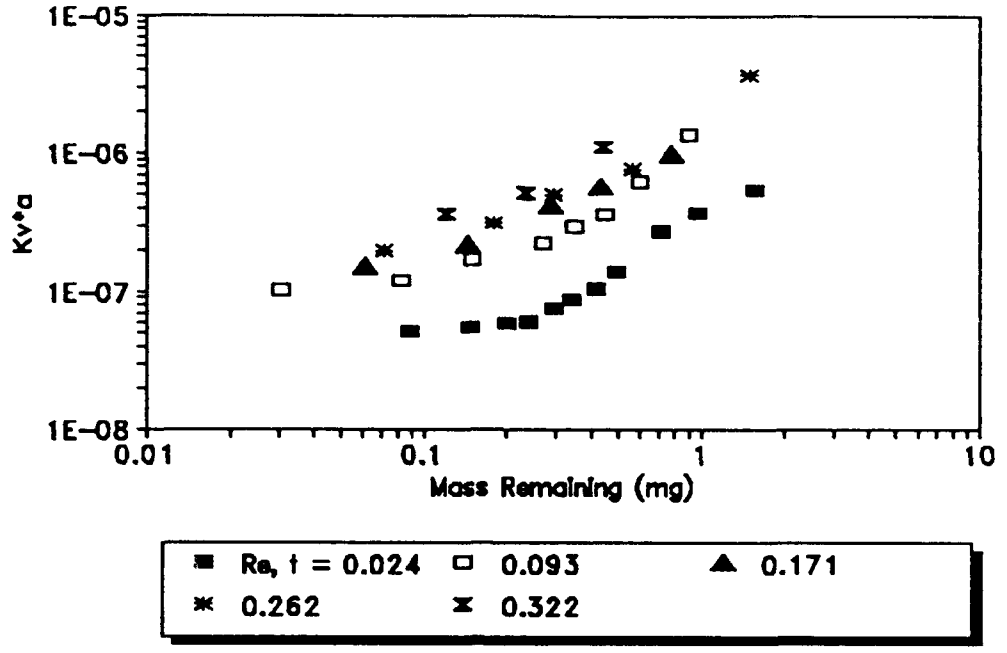


Figure 4.8: A plot of $k_v a$ (moles/$cm^3$-min-mole fraction) versus the mass of heptane remaining in the 80-100 mesh soil column for various terminal modified Reynolds numbers, $Re'_t$.

mechanical dispersion in the pore system - one pore may have heptane, the next may not. The streams are then mixed in a subsequent pore. The overall result is a decrease in the magnitude of the observed $k_v a$.

## 4.4 DETERMINATION OF MASS TRANSFER CORRELATION CONSTANTS

As discussed previously in Section 2.2.2, correlations defining mass transfer coefficients are often determined by fitting experimentally derived data to a power law relationship of the form of Equation 2.12. Since it is compound specific, the Schmidt number (Sc) for this investigation is considered to be constant with a computed magnitude of 2.16 for the temperature conditions of this study. The power of the Schmidt number, c, is also considered to be a constant. The diffusivity, D, of heptane in air was computed from the correlation

of Fuller, Schettler, and Giddings (Tucker and Nelken, 1990) to be 0.079 $cm^2/sec$. The effective pore diameter and the interfacial surface area per bulk volume of bed, $\alpha$, for a given mass of heptane remaining in a given soil column were also considered to be constant. Both sides of Equation 2.9 were multiplied by $\alpha$ and all constants were lumped together resulting in:

$$k_v\alpha = \alpha a(D/d_e)(Re)^b(Sc)^c \quad \text{or} \quad k_v\alpha = a'Re^b \tag{4.1}$$

where: $a' = \alpha a(D/d_e)(Sc)^c$.

The unknown variable, $\alpha$, appears on both sides of this equation. To find a dependance of $k_v\alpha$ on Re, the magnitudes of $\alpha$ and $d_e$ must be held constant for a given bed. Data taken during the constant drying period of each experimental run were regressed to find the dependence of $k_v\alpha$ on the mass of heptane remaining. Computations of Re' were accomplished based on the interstitial pore velocity ($u_v$) and the effective pore diameter. Three values of mass remaining (1, 1.25, and 1.5 grams) which fell within Region 2 for all experimental runs were chosen. Values of $k_v\alpha$ and Re' were calculated from the relationships described above for each value of mass remaining. For every experimental run, regressions of log $k_v\alpha$ versus log Re' were performed for each value of mass remaining for each bed. The regressions of $k_v\alpha$ versus the mass of heptane remaining each yielded one value of $k_v\alpha$ associated with one value of Re' corresponding to a distinct value of mass remaining. The three sets of ordered pairs (log Re', log $k_v\alpha$) corresponding to each bed were regressed to determine the slope (b) and the intercept (log a'). The regressions and corresponding statistical parameters are given in Table 4.1. The regressions are plotted in Figures 4.9 to 4.11.

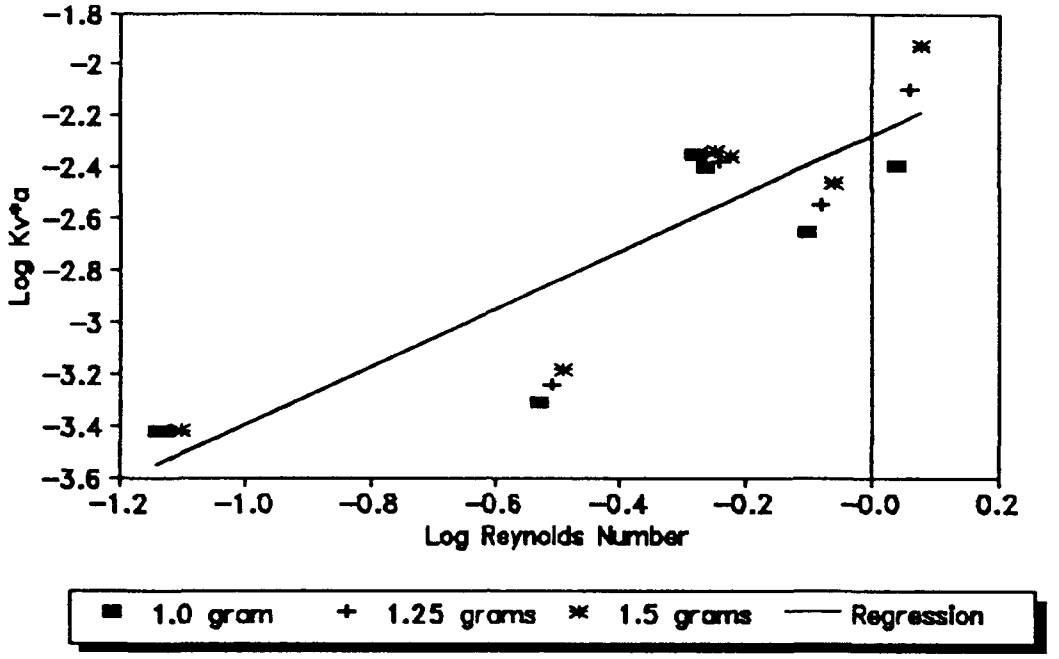


Figure 4.9: A plot of log $k_v a$ versus log Re' for 30/40 mesh soil and three values of mass of heptane remaining in the soil column. Regression line of all data points is shown.

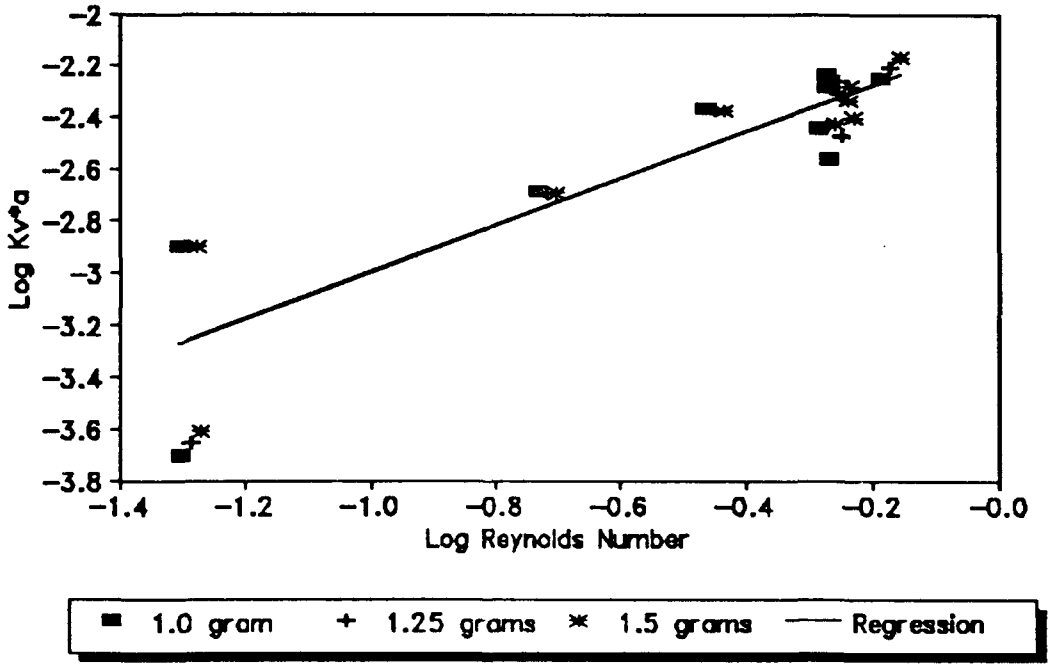


Figure 4.10: A plot of log $k_v a$ versus log Re' for 50/60 mesh soil and three values of mass of heptane remaining in the soil column. Regression line of all data points is shown.

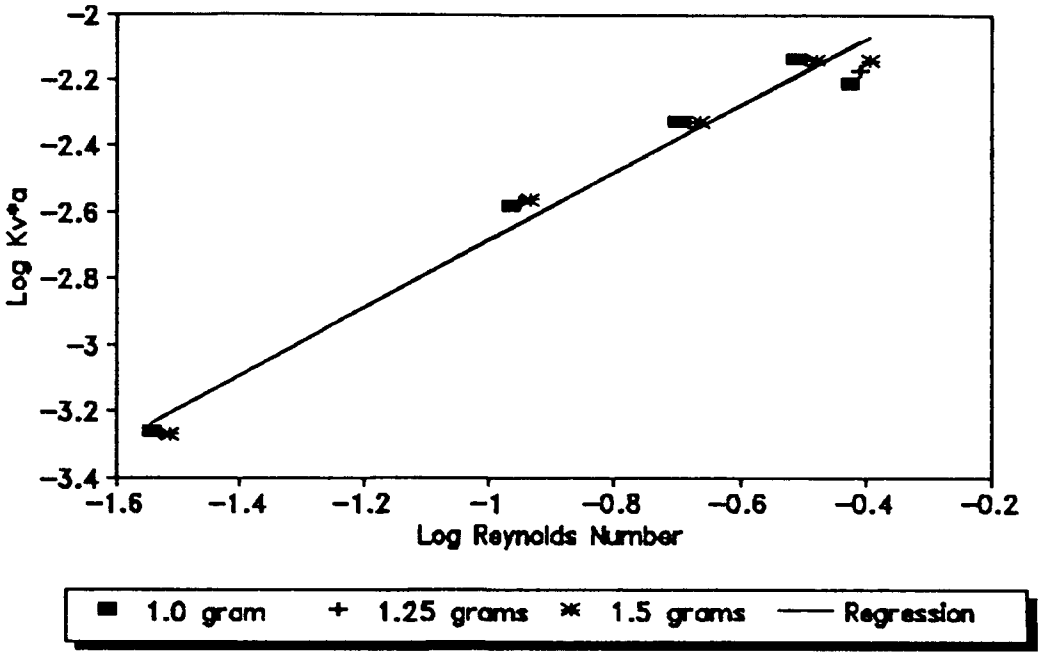


Figure 4.11: A plot of log $k_v a$ versus log Re' for 80/100 mesh soil and three values of mass of heptane remaining in the soil column. Regression line of all data points is shown.

The slopes of these curves ranged from 0.891 to 1.23 with a mean of 1.01 and a standard deviation of 0.11. The intercepts ranged from -1.663 to -2.385. Typical values reported in the literature for the power of the Reynolds number range from 0 (Gamson et al., 1945) to 0.70 (Onda et al., 1968). The results of this study suggest that $k_v$ is indeed dependent on the Reynolds number and that the power of the dependence is on the order of unity.

The nine values of the intercept listed in Table 4.1 constitute nine values of log a'. Unfortunately, the resulting system of equations contains eleven unknowns: nine values of $\alpha$, a, and c. Consequently, the parameters a and c cannot be estimated from the data generated by this investigation. Future efforts must involve the

calculation or experimental determination of $\alpha$, and the use of multiple solutes to determine values for the constants a and c. Computation of $\alpha$ would involve an analytical solution using three-dimensional calculus, the geometry of which would have to be defined. This solution would include: the determination of the contact angle between the organic and solid phases either from the literature or experimentally; an assumption of spherical solid grains; and an assumption of a liquid boundary defined by circular arcs connecting points of tangency at the intersection of the liquid with the solid, revolved about an axis passing through the centers of particles that are in contact. Experimental determination of $\alpha$ would employ compounds of varying surface tension to provide sufficient data to allow additional regression type analyses for verification of the geometrical analysis.

Table 4.1

Regression Results of Log $k_v a$ vs. Log Re'

| Soil Column | Mass (g) Remaining | Slope (b) | Y-intercept (a') | $R^2$ | Significance Level[a] |
|---|---|---|---|---|---|
| 30-40 | 1.0 | 0.972 | -2.385 | 0.699 | 0.025 |
| | 1.25 | 1.133 | -2.264 | 0.796 | 0.01 |
| | 1.5 | 1.233 | -2.194 | 0.834 | 0.01 |
| 50-60 | 1.0 | 0.905 | -2.089 | 0.754 | 0.005 |
| | 1.25 | 0.899 | -2.093 | 0.789 | 0.001 |
| | 1.5 | 0.892 | -2.099 | 0.813 | 0.0005 |
| 80-100 | 1.0 | 1.003 | -1.670 | 0.973 | 0.0005 |
| | 1.25 | 1.020 | -1.666 | 0.981 | 0.0005 |
| | 1.5 | 1.036 | -1.663 | 0.987 | 0.0005 |

[a]From Student's t-test (Dougherty, 1990)

# CHAPTER 5

# SUMMARY, CONCLUSIONS, AND RECOMMENDATIONS FOR FUTURE RESEARCH

## 5.1 SUMMARY

A laboratory system consisting of an ultra-pure air source, a flow-through soil column, a gas chromatograph, and pressure monitoring transducers was developed to study role of mass transfer in the removal of petroleum hydrocarbons from vadose zone soils. The suitability of this system for determination of gas-side mass transfer coefficients was examined. Estimations of the coefficients of mass transfer correlations were made as a function of the convective air flow rate. The soil column is an excellent design to study mass transfer coefficients applicable to the removal of VOCs from soil systems. The analysis of the off-gas using an automated gas sampling loop in line with a gas chromatograph is an ideal method to measure the off-gas concentrations. It was observed, however, that there are differences between the response of the FID to liquid standard samples and off-gas sample introductions. This was quantified as approximately 126% and corrections to the mass balance were made. It was observed that there are three distinct regions of off-gas concentrations over the course of an entire experimental run. Plots of $k_v a$ versus modified Reynolds number (Re') verified these regions. For the constant drying period of each run, the relationship of log $k_v a$ versus Re' resulted in a dependance of $k_v a$ on Re' on the order of Re' to a power of 0.89 to 1.23.

## 5.2 CONCLUSIONS

The major findings of this study are stated as follows:

1) A soil column design, approximating a differential soil bed appears to be an excellent tool for study of mass transfer in the removal of volatile organics from vadose zone soils.

a) The packing arrangement of the soil columns was maintained and no signs of leakage around seals were observed during the course of the study. Experiments were run quickly and efficiently, and connection/disconnection of the column to/from the flow through system presented no problems.

b) Loading of the heptane into the column by vacuum aspiration appeared to be successful. Even distribution of heptane was apparently always achieved.

c) Experimental runs using the same soil bed at nearly the same flows showed very repeatable results.

2) The entire laboratory system (soil column, pressure transducers, data acquisition system (DAS), and GC) appear to be suitable for the experimental measurement of mass transfer coefficients.

a) The pressure transducers were reliable and consistent in providing pressure measurements.

b) The DAS handled the necessary amounts of data with ease.

c) The gas sampling valve and loop seem well suited for rapid, repeatable sampling of soil column off-gas. The response of the flame ionization detector was very linear over the entire analytical range attempted (five orders of magnitude). Some difference exists between the mass-specific responses for sample introduction as a liquid versus a vapor. This difference was measured for n-pentane, and based on these results, the overall

average mass recovery appears to be complete within a few percent.

3) Observed values of $k_v a$ versus Re' do show a dependance of the mass transfer coefficient on a modified Reynolds number.

a) Statistical regression of the data taken during the constant drying period resulted in a dependance of $k_v a$ on Re'.

b) Data observed during a period of constant Re' (Region 3) showed a direct dependence of $k_v a$ on the magnitude of the constant Re' for a given mass of heptane remaining in the soil column.

4) The value of the correlation constant b in $Sh = aRe'^{b}Sc^{c}$ appears to have a value near unity.

a) Regressions of log $k_v a$ versus log Re' at a constant mass of heptane remaining in the soil column resulted in a range of values for the slope (the constant b) of 0.89 to 1.23, a mean value of 1.01, and a standard deviation of 0.11. This compares to a range of values of the power of Re' of 0 to 0.70 suggested in previously published literature.

## 5.3 RECOMMENDATIONS FOR FUTURE RESEARCH

Future experiments using the system developed in this work should use gas standards for calibration of the GC to avoid inaccuracies resulting from differences between the mass-specific responses for liquid and gas sample introduction. Volatilized pure-component or purchased gas standards of lower concentration are the two suggested alternatives. The use of volatilized gas standards would require a system designed to prevent condensation in the off-gas lines prior to the gas sampling loop. Conversely, the use of purchased gas standards

would require extrapolation of standard curves toward higher concentrations for most compounds. Such extrapolation is risky but potentially satisfactory based on the observed linear response of the flame ionization detector.

Future studies should be directed to the separation of $k_v$ from $\alpha$. Three-dimensional calculus and analytical geometry in combination with solid-liquid wetting angle data is one potential means of accomplishing such analysis. Experiments using single components of varying surface tension may also be employed for separation of $k_v$ and $\alpha$, and hence, allowing a somewhat indirect determination of $\alpha$ in addition to verification of the geometric analysis. Future work should focus on the determination of the constants a and c, and further verification of the value of b, in the mass transfer correlation as well.

Studies could then continue with the determination of mass transfer coefficients in binary mixtures of similar and dissimilar molecules. Eventually water, should be introduced into the experiments to assess the effect of this additional, distinct phase on mass transfer in soil venting systems.

## REFERENCES


Agrelot, J.C., J.J. Malot and M.J. Visser, "Vacuum Defense System for Ground Water VOC Contamination," presented at the Fifth National Symposium on Aquifer Restoration and Ground Water Monitoring, Columbus, OH, May 21-24, 1985.

Arbuckle, R.B., "Estimating Activity Coefficients for Use in Calculating Environmental Parameters", Environmental Science and Technology, v. 17, no. 9, 1983, pp 537-542.

Baehr, A.L. and M.Y. Carapcioglu, "A Predictive Model for Pollution of Gasoline in Soils and Groundwater", presented at the Petroleum Hydrocarbons and Organic Chemicals in Groundwater Conference of the National Water Well Association, Houston, TX, November 5-7, 1985.

Baehr, A.L., G.E. Hoag, and M.C. Marley, "Removing Volatile Contaminants from the Unsaturated Zone by Inducing Advective Air-phase Transport", Journal of Contaminant Hydrology, v. 4, 1989, pp 1-26.

Bennedson, M.B., J.P. Scott, and J.D. Hartley, "Use of Vapor Extraction Systems for In Situ Removal of Volatile Organic Compounds from Soil", Proceedings of the National Conference on Hazardous Wastes and Hazardous Materials, HMCRI, 1985, pp 92-95.

Bird, R.B., W.E. Stewart, and E.N. Lightfoot, Transport Phenomena, Wiley, 1960.

Brown, R.A., G. Hoag, and R. Norris, "The Remediation Game: Pump, Dig or Treat?" presented at the Ground Water Quality Protection Pre-Conference Workshop, 61st annual convention of the Water Pollution Control Federation, 1988.

Carman, P.C., Flow of Gases Through Porous Media, Academic Press, 1956.

Chemical Rubber Co., Handbook of Chemistry and Physics, 70th ed., 1989.

Chilton T.H., and A.P. Colburn, "Mass Transfer (Absorption) Coefficients", Industrial and Engineering Chemistry, v. 26, no. 11, 1934, pp 1183-1187.

Chilton T.H., and A.P. Colburn, "Distillation and Absorption in Packed Columns", Industrial and Engineering Chemistry, v. 27, no. 3, 1935, pp 255-260.

Davis, B.L., "Particle Shape Factor Analysis", unpublished instructional handout, South Dakota School of Mines and Technology, March 1991.

DePaoli, D.W., S.E. Herbes and M.G. Elliot, "Performance of *In Situ* Soil Venting System at Jet Fuel Spill Site," presented at the U.S. EPA Soil Vapor Extraction Workshop, Edison, NJ, June 28-29, 1989.

Dougherty, E.R., Probability and Statistics for the Engineering, Computing, and Physical Sciences, Prentice Hall, Inc., 1990.

Downey, D.C., and M.G. Elliot, "Performance of Selected *In Situ* Decontamination Technologies: An Air Force Perspective", presented at the American Institute of Chemical Engineeers Summer National Meeting, Philadelphia, PA, August 20-23, 1989.

Dullien, F.A.L., Porous Media - Fluid Transport and Pore Structure, Academic Press, 1979.

Environmental Protection Agency, SITE Technology Demonstration Summary, EPA/540/S5-89/003, 1989a.

Environmental Protection Agency, "Terra Vac *In Situ* Vacuum Extraction System, Applications Analysis Report," EPA/540/A5-89/003, 1989b.

Freeze, R. A. and J.A. Cherry, Groundwater, Prentice-Hall, Inc., 1979.

Gamson, B.W., G. Thodos, and O.A. Hougen, "Heat, Mass, and Momentum Transfer in the Flow of Gases Through Granular Solids", Trans. of The American Institute of Chemical Engineers, v. 39, 1943, pp 1-35.

Gierke, J.S., N.J. Hutzler, and J.C. Crittenden, "Modeling the Movement of Volatile Organic Chemicals in Columns of Unsaturated Soil", accepted for publication by Water Resources Research, 1989.

Grain, C.F., "Activity Coefficients", chapter 11, Lyman, W.J., W.F. Reehl and D.H. Rosenblatt, eds., Handbook of Chemical Property Estimation Methods, American Chemical Society, 1990.

Henley, E.J. and J.D. Seader, Equilibrium-Stage Separations in Chemical Engineering, Wiley, 1981.

Hunt, J.R., N. Sitar, and K.S. Udell, "Nonaqueous Phase Liquid Transport and Cleanup - 1. Analysis of Mechanisms", Water Resources Research, v. 24, no. 8, August 1988, pp 1247-1258.

Hutzler, N.J., J.S. Gierke and L.C. Krause, Movement of Volatile Organic Chaemicals in Soils, Soil Science Society of America and American Society of Aronomy, 1989a.

Hutzler, N.J., B.E. Murphy and J.S. Gierke, "State of Technology Review, Soil Vapor Extraction Systems," Cooperative Agreement CR-814319-01-1, EPA ORD, 1989b.

Johnson, P.C., M.W. Kemblowski, and J.D. Colthart, "Quantitative Analysis for the Clean-up of Hydrocarbon-Contaminated Soils by In-situ Soil Venting", Shell Development Publication, 1990, pp 5.5.1-5.5.50.

Lamarche, P. and R.L. Droste, "Air-Stripping Mass Transfer Correlations for Volatile Organics", Journal of the American Water Well Association, January 1989, pp 78-89.

Lisiecki, J.B. and F.C. Payne, "Soil Vapor Recovery Technology," presented at Superfund '89, HMCRI, Washington, D.C., November 27-29, 1989.

Lyman, W.J., "Solubility of Various Solvents", chapter 3, Lyman, W.J., W.F. Reehl and D.H. Rosenblatt, eds., Handbook of Chemical Property Estimation Methods, American Chemical Society, 1990.

Marley, M.C., and G.E. Hoag, "Induced Soil Venting for Recovery/Restoration of Gasoline Hydrocarbons in the Vadose Zone", National Water Well Association/American Petroleum Institute Conference, Houston, TX, November 5-7, 1984.

Mutch, R.D., Jr., A.N. Clarke, J.H. Clarke and D.J. Watson, "*In Situ* Vapor Stripping: Preliminary Results of a Field-Scale U.S. EPA/ Industry Funded Research Project," proceedings of Superfund '89, HMCRI, Washington, D.C., November 27-29, 1989.

Onda, K., H. Takeuchi, and Y. Okumoto, "Mass Transfer Coefficients Between Gas and Liquid Phases in Packed Columns", Chemical Engineering Journal of Japan, v. 1, no. 1, 1968, p 56.

Perloff, W.H. and W. Baron, Soil Mechanics, Ronald Press, 1976.

Perry, R.H., D.W. Green, and J.O. Maloney, eds., Perry's Chemical Engineer's Handbook, 6th ed., McGraw-Hill, 1984

Rogers, J.A., and M. Kaviany, "Variation of Heat and Mass Transfer Coefficients During Drying of Granular Beds", Trans. of the American Society of Mechanical Engineers, v. 112, August 1990, pp 668-674.

Sleep, B.E., and J.F. Sykes, "Modeling the Transport of Volatile Organics in Variably Saturated Media", Water Resources Research, v. 25, no. 1, January 1989, pp 81-92.

Treybal, R.E., Mass Transfer Operations, McGraw-Hill, 1980.

Tucker, W.A., and L.H. Nelken, "Diffusion Coefficients in Air and Water", chapter 17, Lyman, W.J., W.F. Reehl and D.H. Rosenblatt, eds., Handbook of Chemical Property Estimation Methods, American Chemical Society, 1990.

Wilke, C.R. and O.A. Hougen, "Mass Transfer in the Flow of Gases Through Granular Solids Extended to Low Modified Reynolds Numbers", Trans. of the American Institute of Chemical Engineers, v. 41, 1945, pp 445-451.

# APPENDIX A

# OFF-GAS HEPTANE CONCENTRATION PROFILES

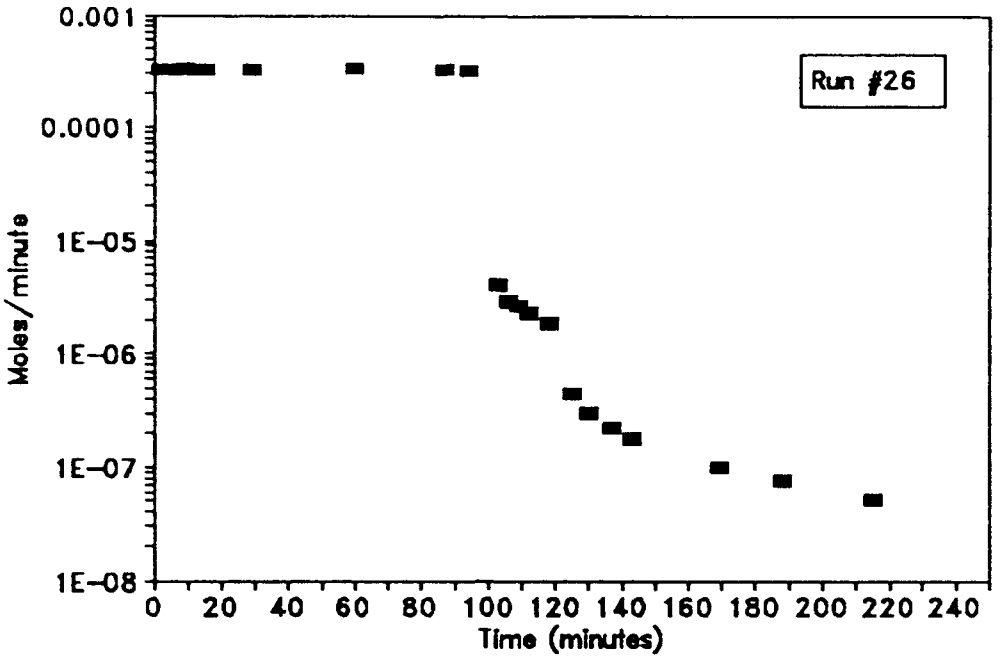


Figure A.1: Off-gas concentration (moles heptane/min) versus elapsed experimental run time for 30/40 mesh soil and a terminal pore velocity ($U_t$) of 0.295 cm/sec.

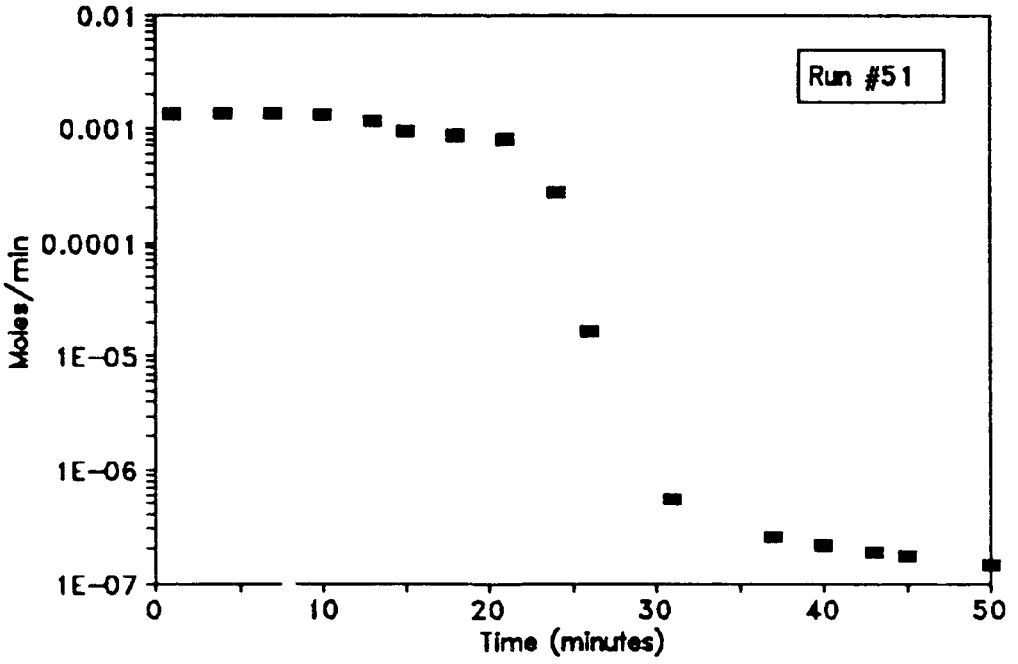


Figure A.2: Off-gas concentration (moles heptane/min) versus elapsed experimental run time for 30/40 mesh soil and a terminal pore velocity ($U_t$) of 1.10 cm/sec.

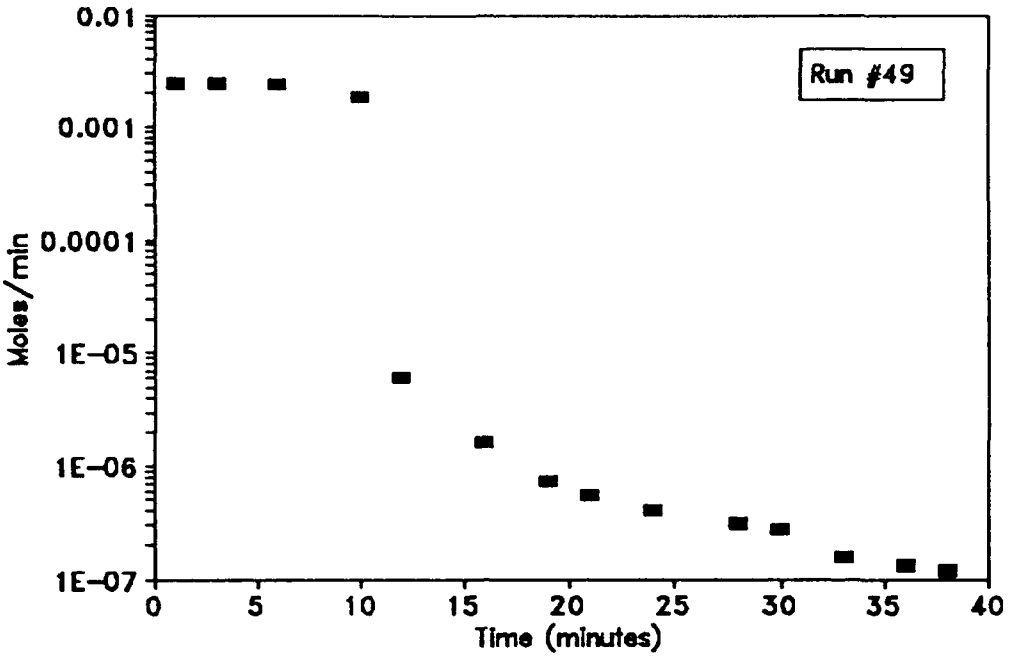


Figure A.3: Off-gas concentration (moles heptane/min) versus elapsed experimental run time for 30/40 mesh soil and a terminal pore velocity ($U_t$) of 1.83 cm/sec.

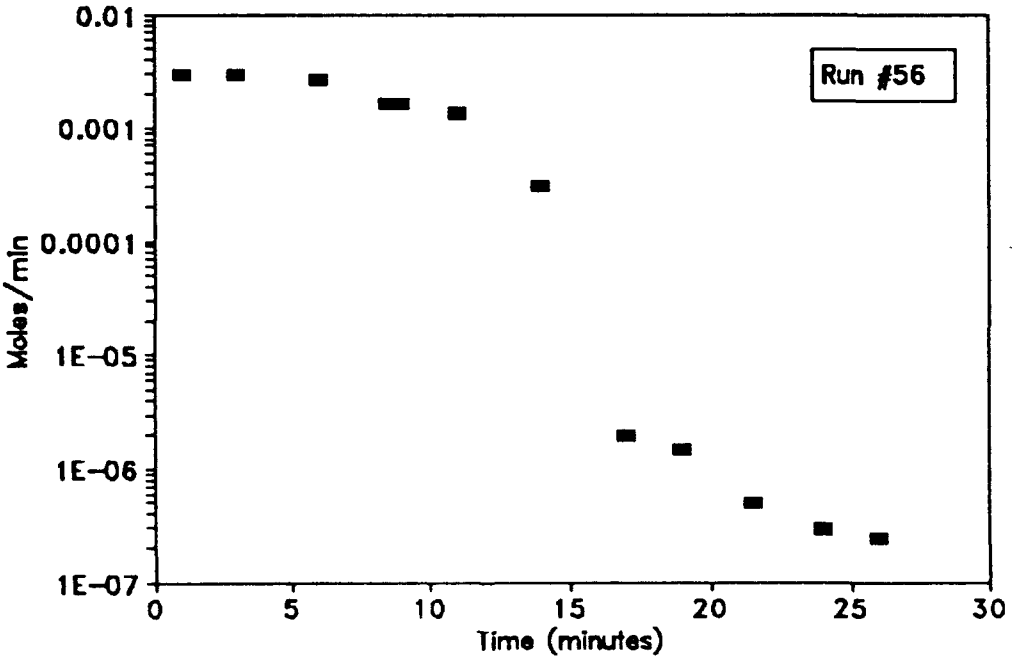


Figure A.4: Off-gas concentration (moles heptane/min) versus elapsed experimental run time for 30/40 mesh soil and a terminal pore velocity ($U_t$) of 2.07 cm/sec.

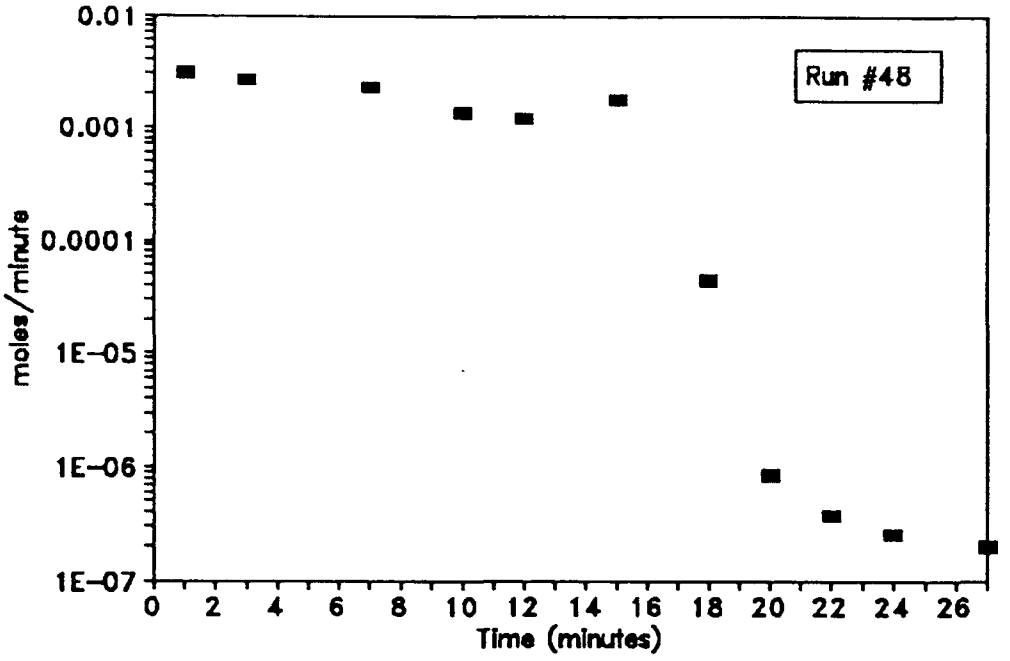


Figure A.5: Off-gas concentration (moles heptane/min) versus elapsed experimental run time for 30/40 mesh soil and a terminal pore velocity ($U_t$) of 2.40 cm/sec.

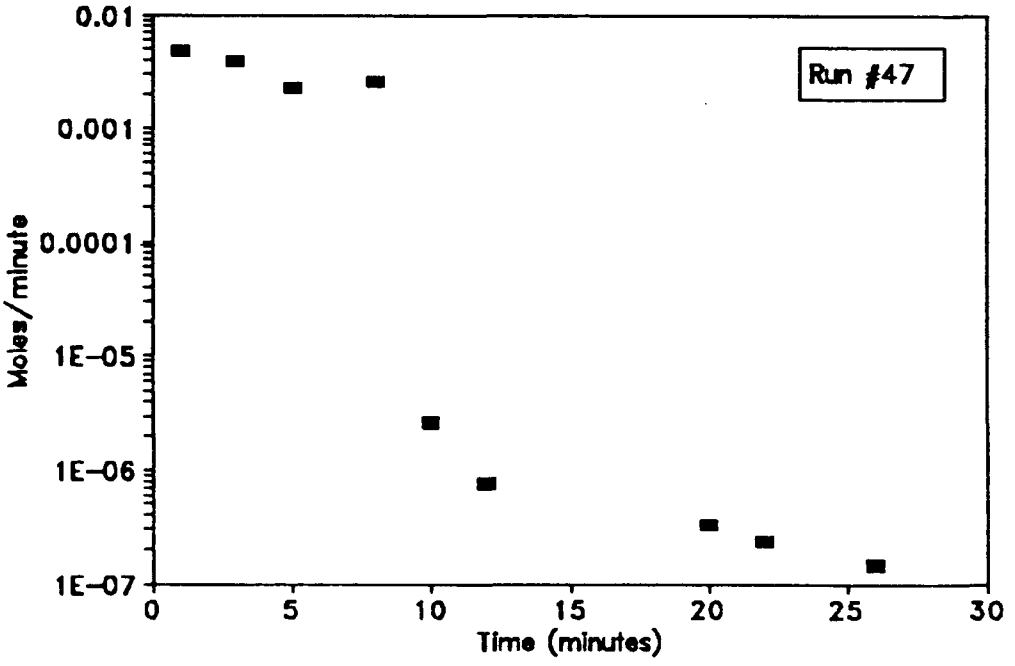


Figure A.6: Off-gas concentration (moles heptane/min) versus elapsed experimental run time for 30/40 mesh soil and a terminal pore velocity ($U_t$) of 2.58 cm/sec.

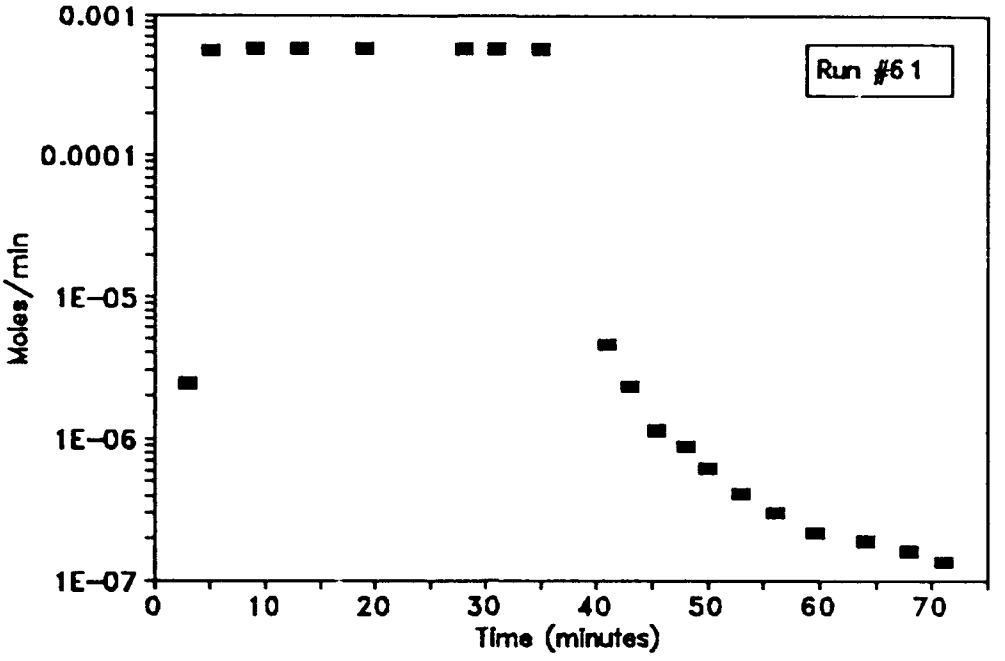


Figure A.7: Off-gas concentration (moles heptane/min) versus elapsed experimental run time for 50/60 mesh soil and a terminal pore velocity ($U_t$) of 0.349 cm/sec.

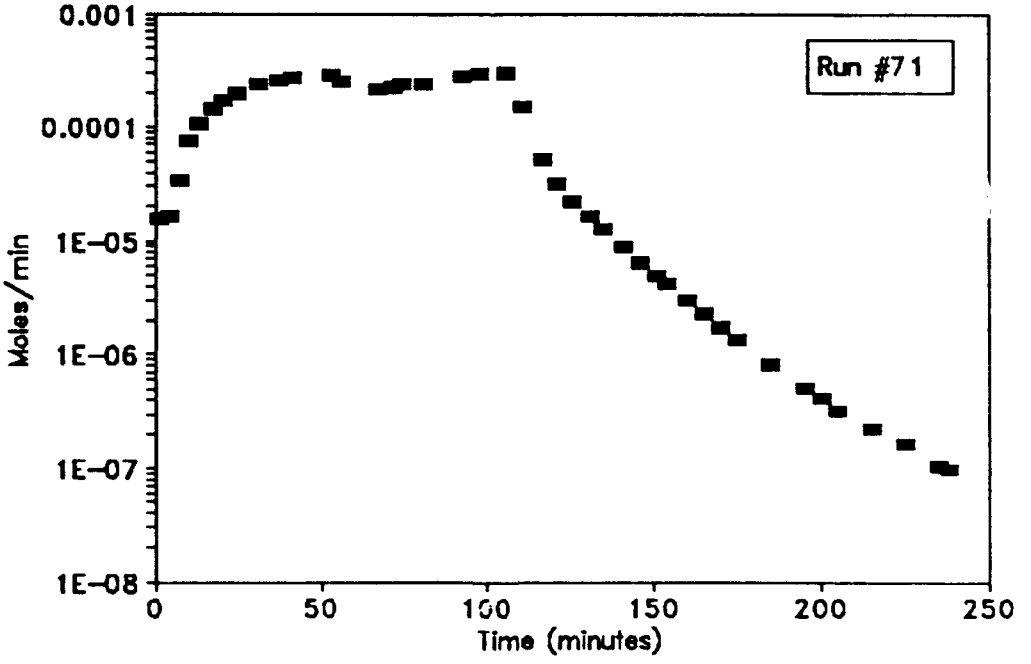


Figure A.8: Off-gas concentration (moles heptane/min) versus elapsed experimental run time for 50/60 mesh soil and a terminal pore velocity ($U_t$) of 0.359 cm/sec.

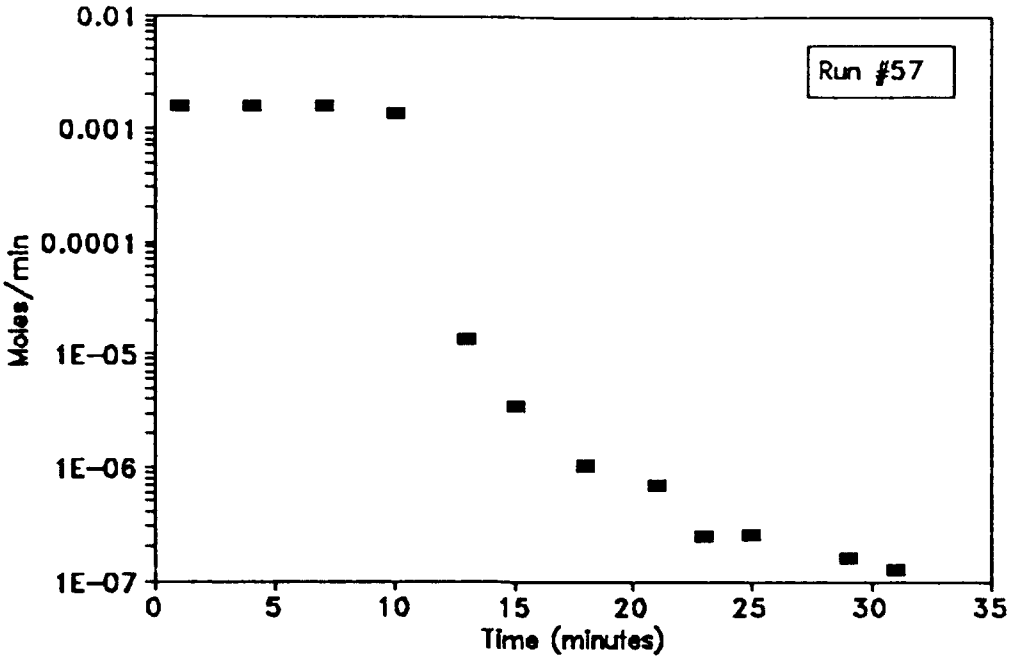


Figure A.9: Off-gas concentration (moles heptane/min) versus elapsed experimental run time for 50/60 mesh soil and a terminal pore velocity ($U_t$) of 1.29 cm/sec.

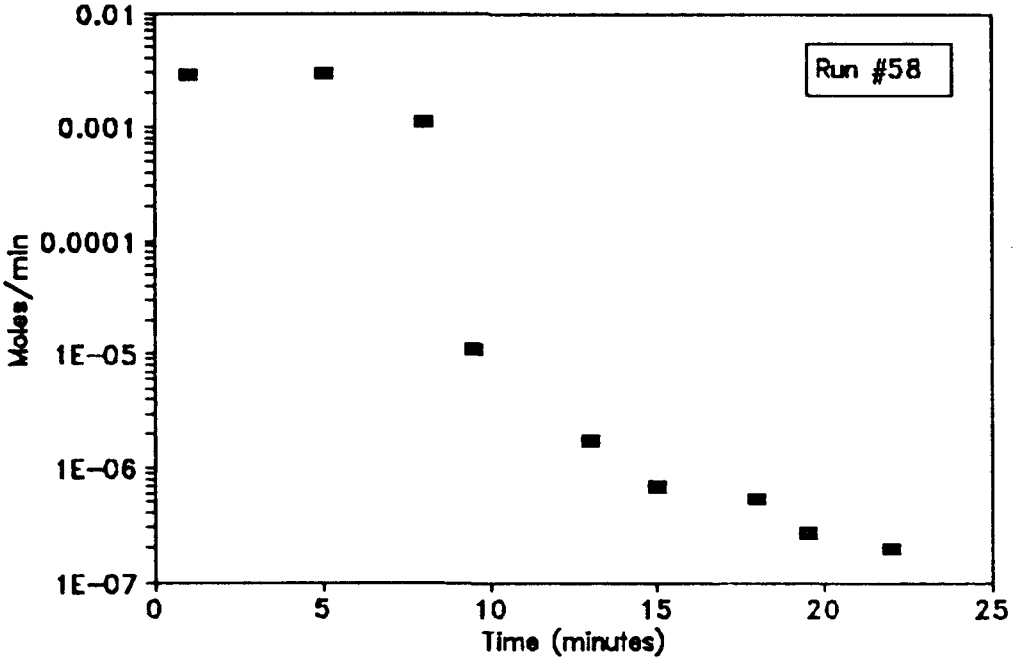


Figure A.10: Off-gas concentration (moles heptane/min) versus elapsed experimental run time for 50/60 mesh soil and a terminal pore velocity ($U_t$) of 2.25 cm/sec.

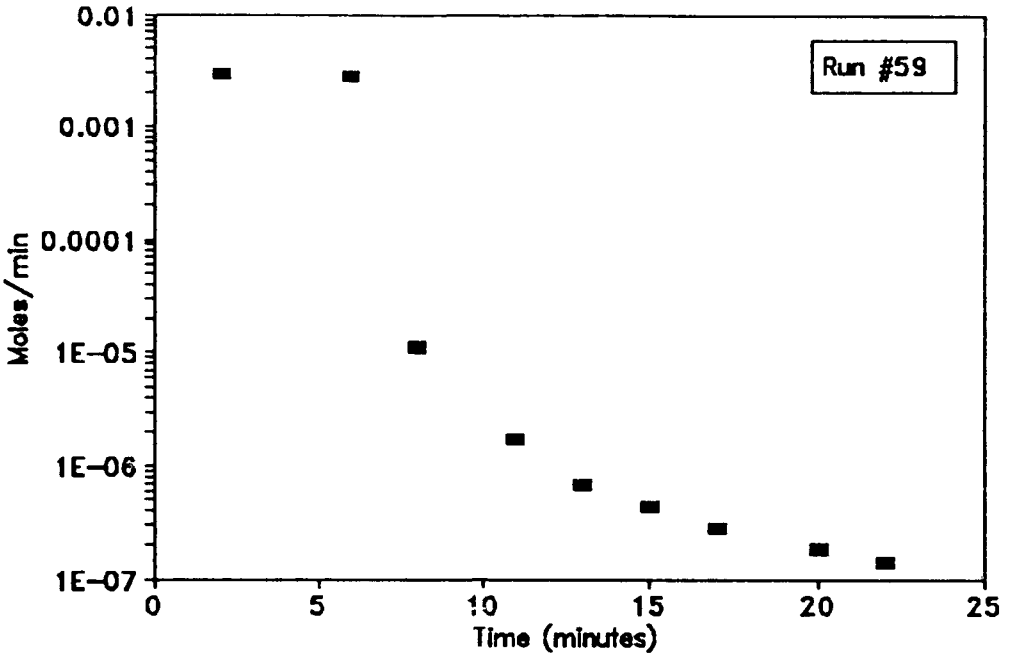


Figure A.11: Off-gas concentration (moles heptane/min) versus elapsed experimental run time for 50/60 mesh soil and a terminal pore velocity ($U_t$) of 3.22 cm/sec.

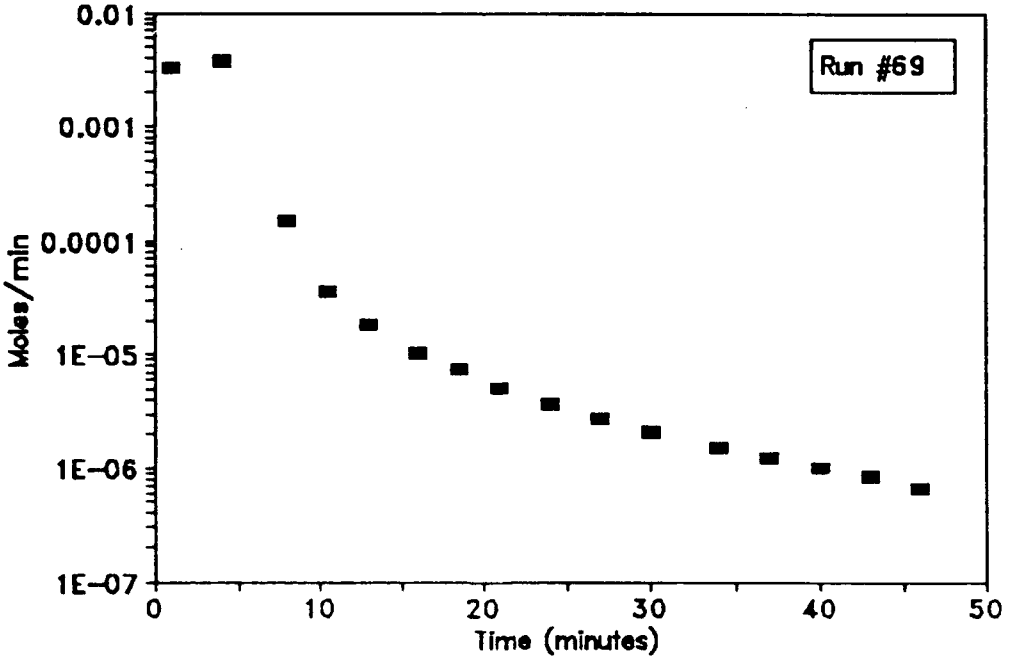


Figure A.12: Off-gas concentration (moles heptane/min) versus elapsed experimental run time for 50/60 mesh soil and a terminal pore velocity ($U_t$) of 3.24 cm/sec.

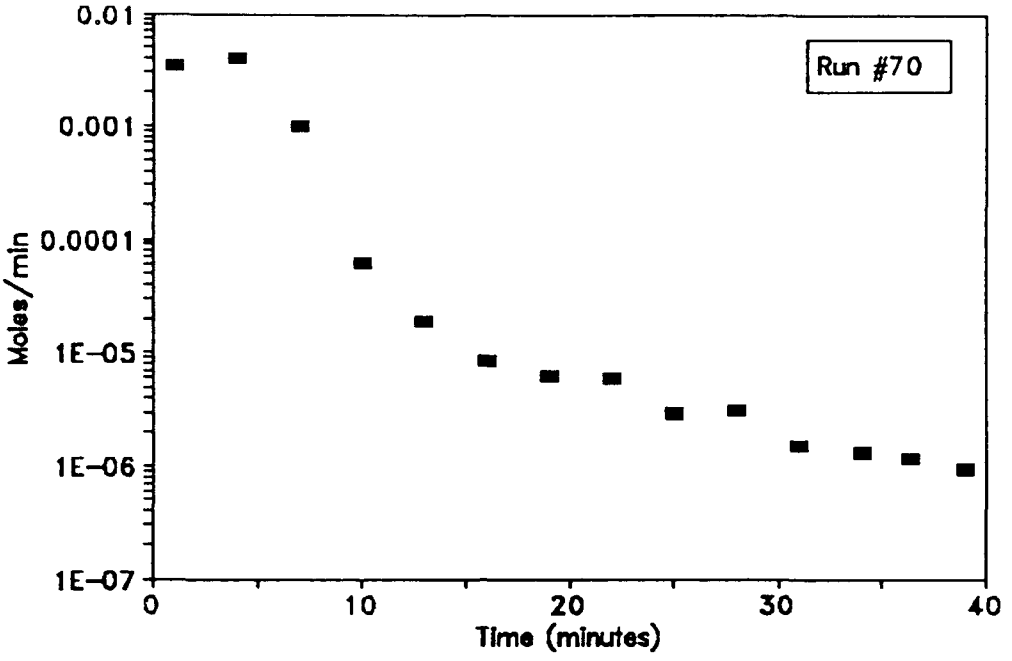


Figure A.13: Off-gas concentration (moles heptane/min) versus elapsed experimental run time for 50/60 mesh soil and a terminal pore velocity ($U_t$) of 3.25 cm/sec.

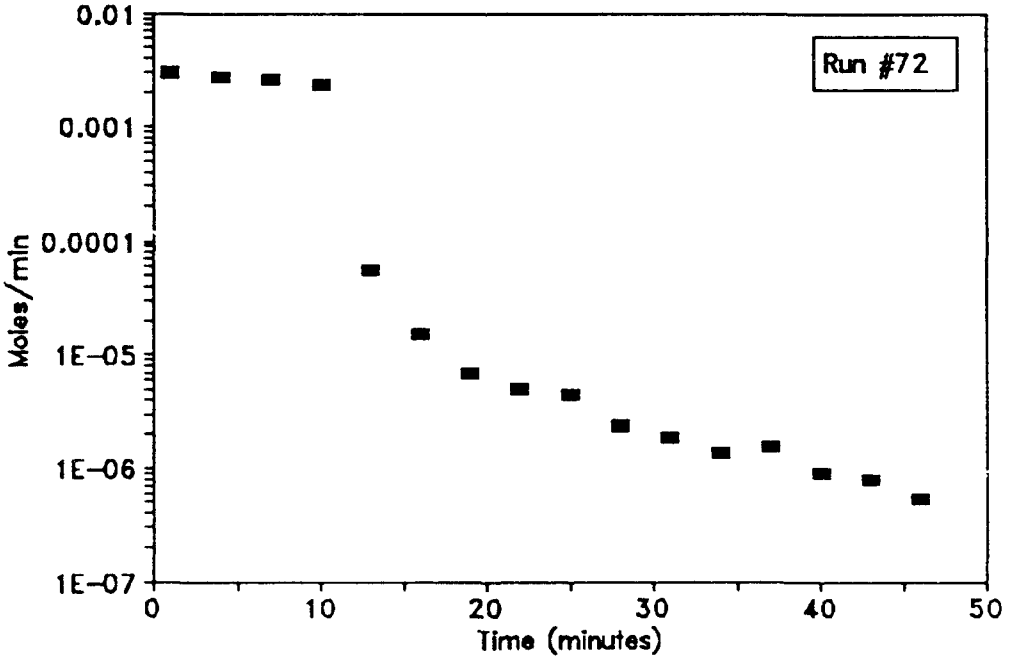


Figure A.14: Off-gas concentration (moles heptane/min) versus elapsed experimental run time for 50/60 mesh soil and a terminal pore velocity ($U_t$) of 3.27 cm/sec.

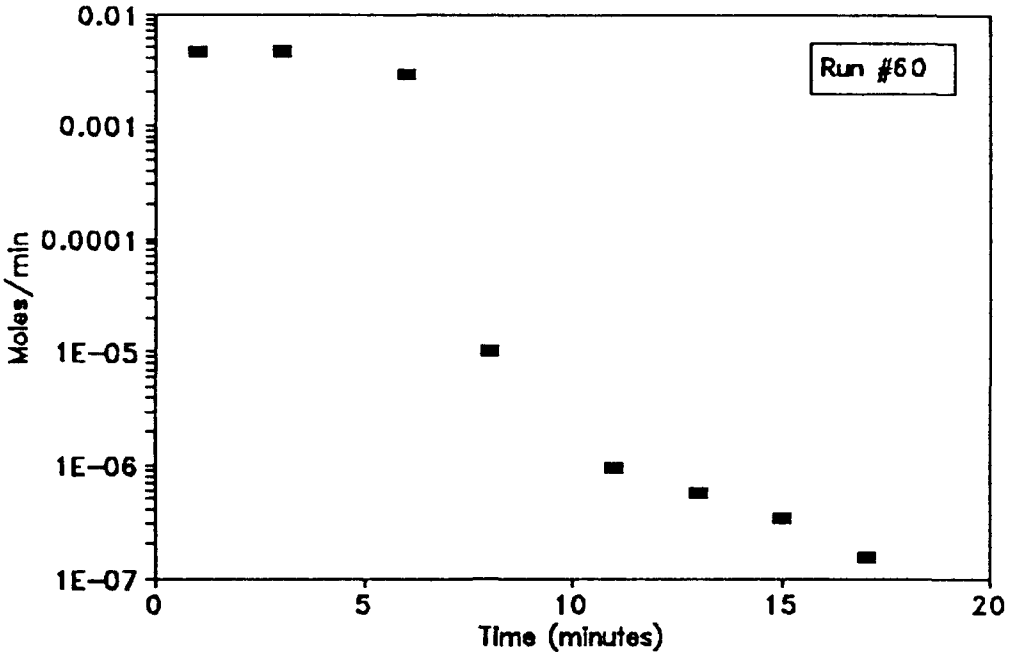


Figure A.15: Off-gas concentration (moles heptane/min) versus elapsed experimental run time for 50/60 mesh soil and a terminal pore velocity ($U_t$) of 3.74 cm/sec.

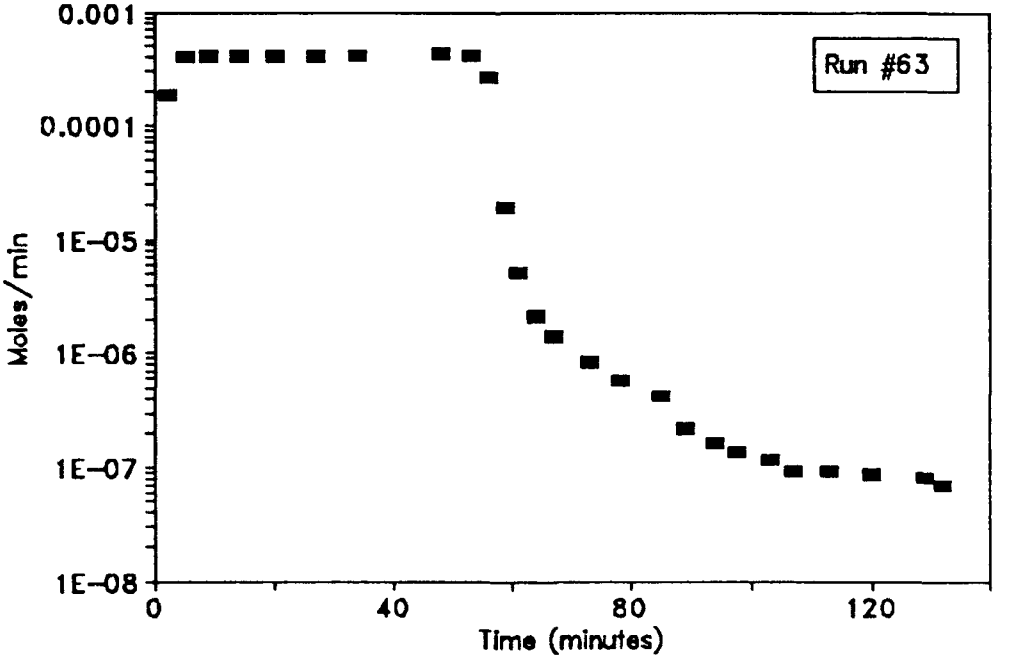


Figure A.16: Off-gas concentration (moles heptane/min) versus elapsed experimental run time for 80/100 mesh soil and a terminal pore velocity ($U_t$) of 0.333 cm/sec.

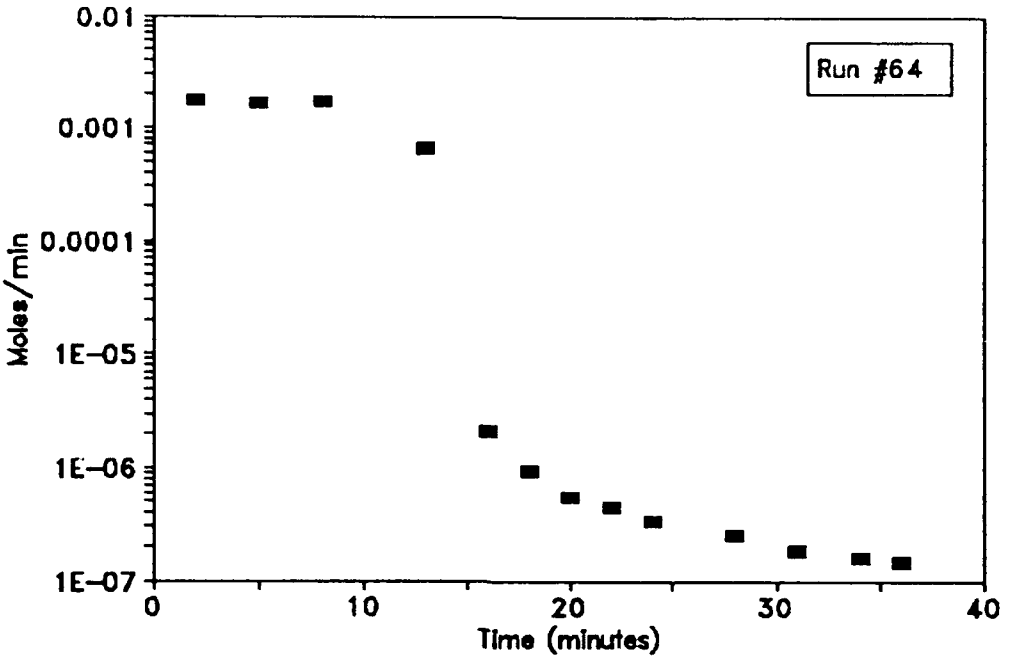


Figure A.17: Off-gas concentration (moles heptane/min) versus elapsed experimental run time for 80/100 mesh soil and a terminal pore velocity ($U_t$) of 1.23 cm/sec.

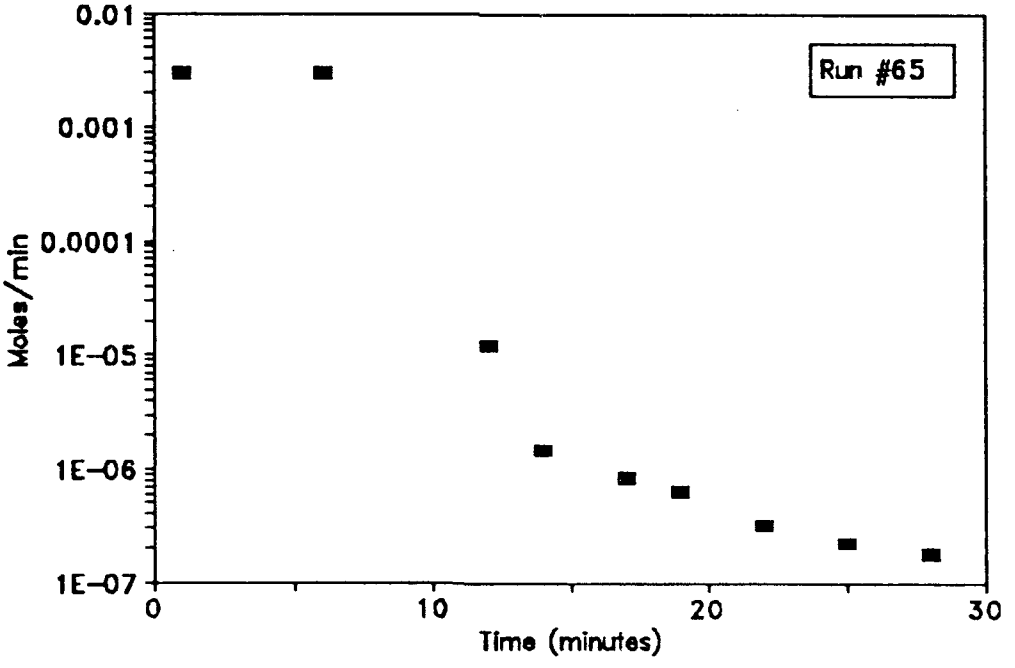


Figure A.18: Off-gas concentration (moles heptane/min) versus elapsed experimental run time for 80/100 mesh soil and a terminal pore velocity ($U_t$) of 2.15 cm/sec.

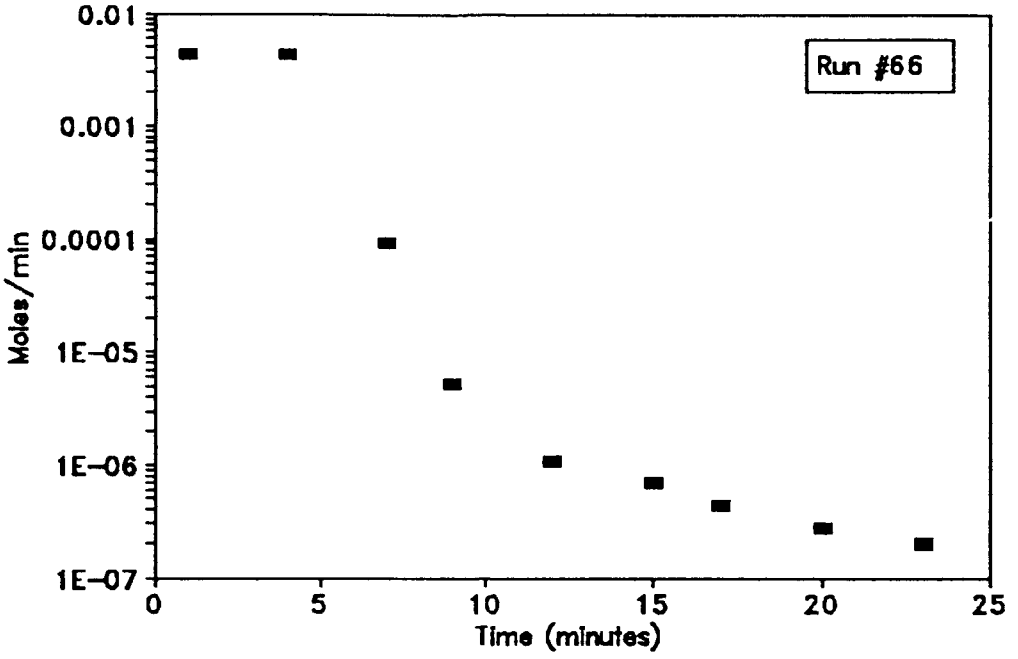


Figure A.19: Off-gas concentration (moles heptane/min) versus elapsed experimental run time for 80/100 mesh soil and a terminal pore velocity ($U_t$) of3.08 cm/sec.

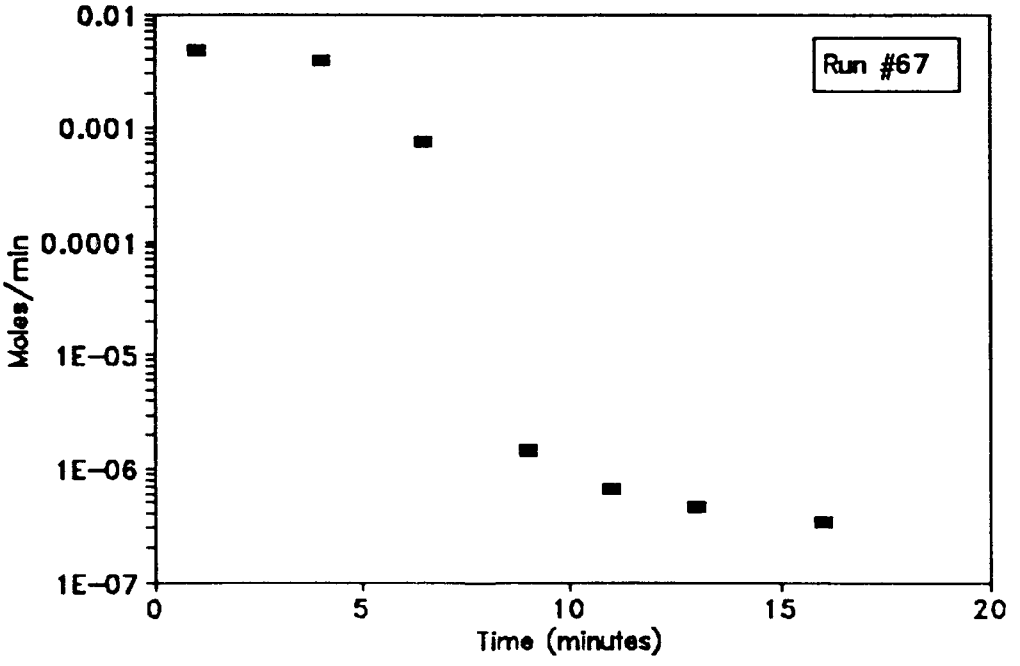


Figure A.20: Off-gas concentration (moles heptane/min) versus elapsed experimental run time for 80/100 mesh soil and a terminal pore velocity ($U_t$) of 3.53 cm/sec.

## Vita

Michael Van Valkenburg was born in West Point, New York on October 23, 1963. He received his Bachelor of Science degree in Chemical Engineering from Washington University in Saint Louis in May 1985. He was commissioned as a United States Air Force officer during the same month. He served as a Bioenvironmental Engineer from June 1985 until June 1987 at Williams AFB, Arizona and at Ellsworth AFB, South Dakota from June 1987 until August 1989. In these positions he managed the Air Force's Industrial Hygiene and Environmental Protection programs for the two Air Force bases. Since August of 1989 he has been a graduate student at the South Dakota School of Mines and Technology, and upon graduation, Captain Van Valkenburg will be an Instructor of Chemistry at the United States Air Force Academy, Colorado.